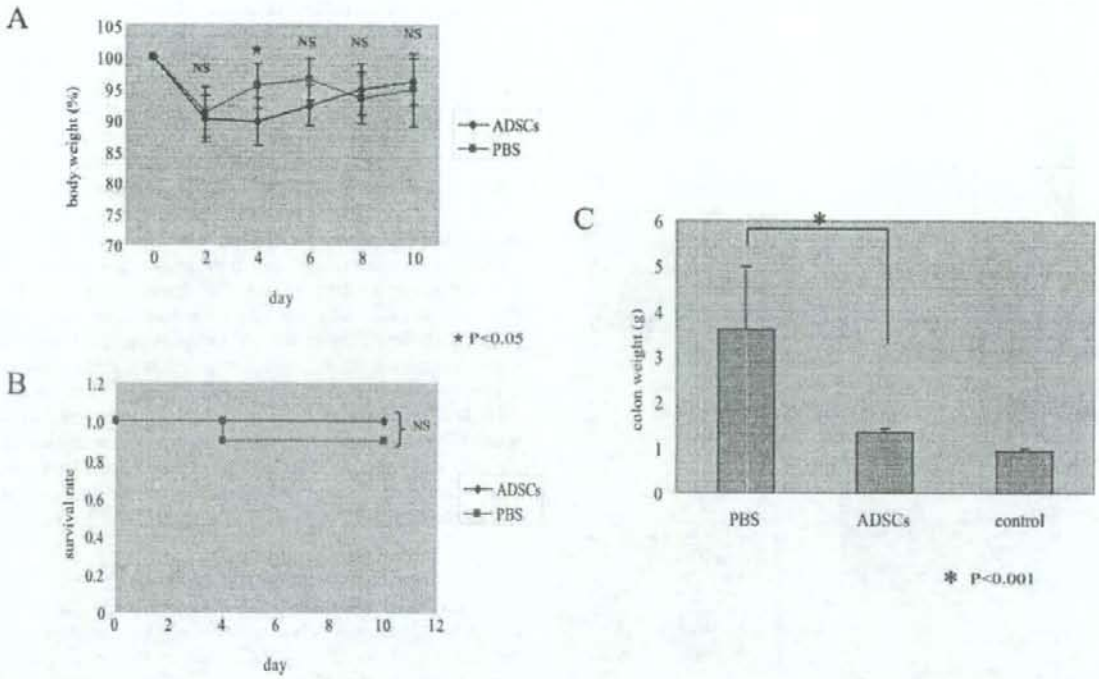

FIGURE 7. Measurement of body and colonic weight and survival rate after inoculating the colitis-model rats with ADSCs. A: Body weight was measured every 2 days, and colonic weight was determined 8 days after the injection of ADSCs (10 days after the injection of TNBS). It is noted that there was no statistically significance difference in body weight between the recipients of PBS and the recipients of ADSCs (except on day 4). B: Effects of ADSCs on survival rate were examined. Statistical analysis was performed by the log rank test. C: Colonic weight was measured 8 days after the submucosal injection of ADSCs. The results are representative of 2 replicate experiments. Symbols, columns, and bars represent the means ± SDs of 10 rats ($^*P < 0.001$).

ulcers and colon length were measured (Fig. 8A). As shown in Figure 8B, the ulcer area was significantly reduced (23 ± 2 mm^2) in the TBNS-induced-colitis rats treated with ADSCs compared with those treated with PBS (65 ± 13 mm^2; $P < 0.05$). However, there was no statistically significant difference in colonic length between the rats treated with ADSCs (15.2 ± 0.2 cm) and the rats treated with PBS (15.3 ± 0.8 cm; Fig. 8C). Furthermore, we evaluated the proliferation of colonic epithelium (photographed in Fig. 8D,E) by the injection of BrdU. When the colitis-induced rats were treated with ADSCs, the number of BrdU-positive cells significantly increased in the mucosal epithelium surrounding colonic ulcers when compared with those treated with PBS (treated with ADSCs, 28.1 ± 3.6/crypt, versus treated with PBS, 18.9 ± 4.0/crypt; $P < 0.05$; Fig. 8F).

Inoculation of ADSCs Ameliorates Colitis

Histological examination was carried out to determine whether ADSCs could reduce the inflammation induced by TNBS. Extensive ulceration with coagulative necrosis extending into the muscularis propria was observed in the untreated (PBS-injected) group, and numerous neutrophils (and relatively small numbers of mononuclear cells) were detected as inflammatory cells (Fig. 9A). In contrast with these findings, in the group injected with ADSCs, a decrease in the infiltration of inflammatory cells was clearly observed along with amelioration of edema and the concomitant enhancement of epithelial regeneration, as shown in Figure 9B. Histological score is summarized in Figure 9C.

MPO activity, an index of inflammatory response, was next determined in the colon in order to evaluate the degree of inflammation in the rats treated with ADSCs or PBS after the induction of colitis by TNBS. A significant increase in MPO activity was observed in the injured colon of colitis-model rats, and the injection of ADSCs (but not PBS) was able to reduce the local MPO activity (Fig. 9D). In addition, other inflammatory cytokines, such as TNF-α, IFN-γ, IL-1β,

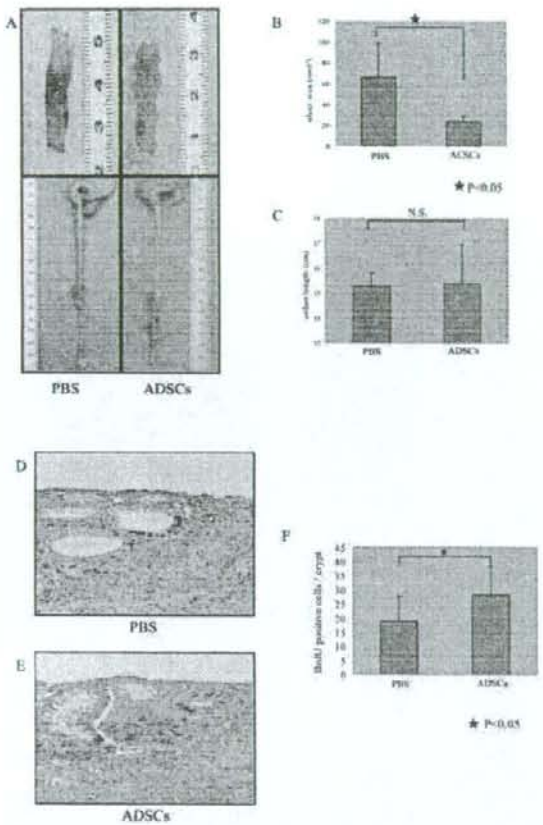

FIGURE 8. Effects of ADSCs in the repair of colonic ulcer. ADSCs or PBS submucosally injected into colitis-induced rats. A: Macroscopic examination of the area of colonic ulcers and the colon 8 days after the submucosal injection of ADSCs or PBS. B: Area of the ulcer was measured using NIH image software on pictures of the colon. C: Length (colocecal junction to anal verge) of the colon was measured by a scale. D, E: Proliferation of colonic epithelial cells was measured by injection of BrdU into rats treated with ADSCs or PBS. Representative photographs of PBS and ADSCs are shown in D and E, respectively (magnification ×400). F: BrdU-positive cells were counted, and the number of positive cells per crypt was calculated. Columns and bars represent the means ± SDs of 10 rats.

and IL-8, were examined. The expression of GRO/CINC-1 (functionally equivalent to IL-8), but not of IL-1β, TNF-α, or IFN-γ was reduced by the injection of ADSCs into the colitis-model rats (data not shown). These findings clearly show that ADSCs can ameliorate an inflammatory reaction and reduce the level of some inflammatory cytokines induced by the injection of TNBS.

Distribution and Differentiation of ADSCs In Vivo

We carried out ex vivo studies to determine whether ADSCs can differentiate into the colonic mucosa. We examined the presence of ADSCs (or ADSC-derived cells) submucosally injected by tracing Y-chromosome-positive cells with FISH (Fig. 10A–E). When compared with normal uninjured mucosal area, more than 3 times the number of ADSCs were detected in the ulcer area (22.2 ± 4.7 versus 54.4 ± 17.4 cells/field, $P < 0.05$; Fig. 10F). Most of the ADSCs were observed in the submucosal layer, whereas some were observed in the mucosal layer and in the muscularis propria. No Y-chromosome-positive cells (ADSC-derived cells) were observed in the epithelial cells, vessel component, or nerve cells (data not shown). Furthermore, Y-chromosome-positive cells were determined after staining with cytokeratin, vimentin, S-100, or SMA in order to characterize cells of ADSC origin (Fig. 11). Y-chromosome-positive cells were detected in fibroblast-like cells under the basal membrane, in smooth muscle cells in the muscle layer, and in adipose tissue. However, they were not detected in endothelial cells, the neural crest, and epithelial cells.

DISCUSSION

In the present study, we have shown that ADSCs can facilitate colonic mucosal repair and reduce the infiltration of inflammatory cells. The ADSCs used in the present study were characterized as $CD90^+CD45^-$ cells,[15,16] being similar to bone marrow–derived mesenchymal stem cells (MSCs),[1,3,4,7] and they were cytohistochemically confirmed to be functional MSCs (Figs. 4 and 5) because of their capacity to differentiate into cells with adipogenic, osteogenic, neurogenic, and epitheliogenic lineages when lineage-specific induction factors have been added to the culture, as has been previously reported.[2,9,17,18] Therefore, the ADSCs used in the present study have similar features to MSCs from the bone marrow. The proliferative capacity of the ADSCs was also similar to that of MSCs.[4,7,15,16] The doubling time of ADSCs remained unchanged until 10 passages (Fig. 3). Therefore, along with the ADSCs being easily obtained by lipoaspiration,[19] ADSCs can be a useful candidate for the source of cell therapy.

In addition, one advantage of ADSCs is their potential to secrete growth factors, such as VEGF, HGF,[20] and adiponectin,[21] which facilitate the regeneration of injured tissue alone or synergistically.[22] As has been reported, HGF regulates cell growth, motility, and morphogenesis of various types of cells, including epithelial cells and endothelial cells, and it also prevents fibrosis.[23,24] Recent studies have shown that the combination of HGF with VEGF increases neovascularization in the rat corneal assay[25] and that HGF facilitates the repair of large colonic ulcers in TNBS-induced colitis in rats.[26] Adiponectin has been reported to not only improve insulin resistance and prevent atherosclerosis, fatty liver, and

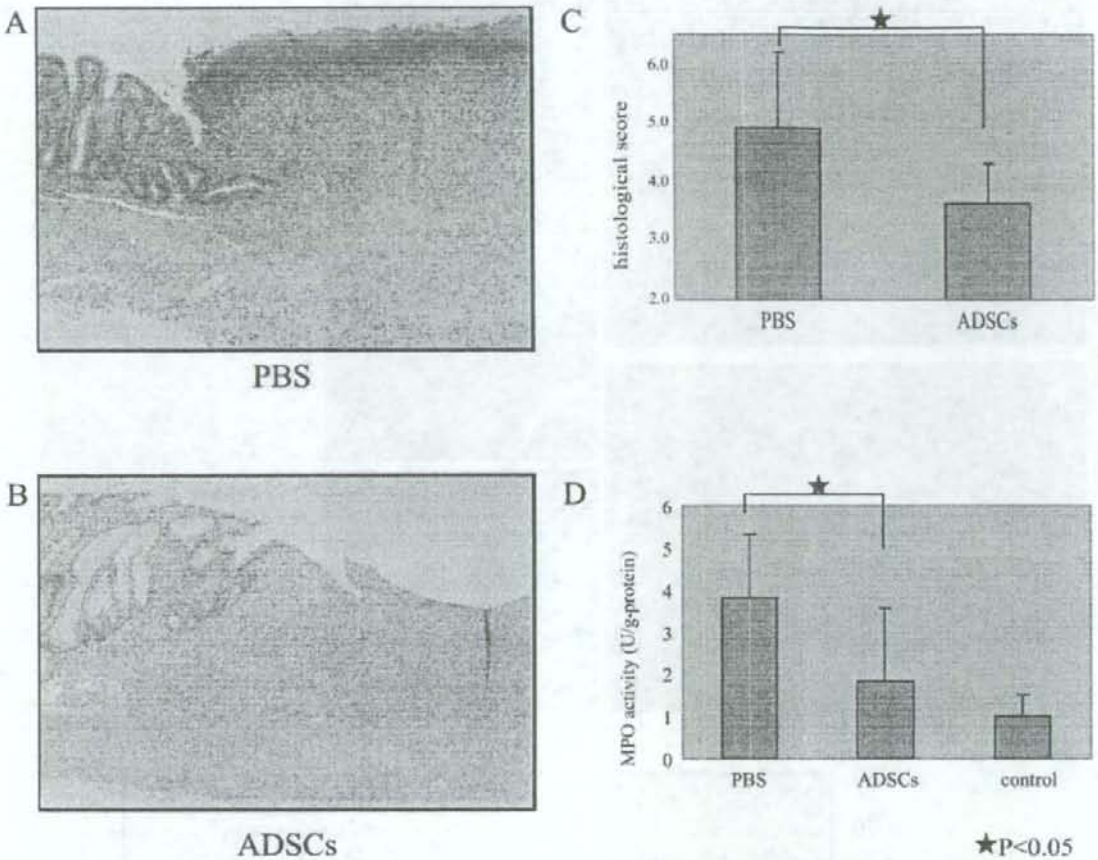

FIGURE 9. Amelioration of colitis and reduction of inflammatory responses by ADSCs. A: Histopathologic examination of colon was carried out in TNBS-induced colitis rats injected with PBS. It is noted that extensive mucosal damage and marked inflammatory cell infiltration were observed. B: Histopathologic examination of colon 8 days after injection of ADSCs; the development of regenerative epithelium, and reduced inflammatory cell infiltration and edema were observed (magnification ×100). C: Histological score of rats injected with PBS or ADSCs. D: Measurement of MPO activity. Colonic MPO activity determined 10 days after injection of PBS or ADSCs in colitis-induced rats. The rats injected with PBS alone (without injection of TNBS or ADSCs) served as controls. Columns and bars represent the means ± SDs of 10 rats ($^*P < 0.05$).

liver fibrosis but also to exert several anti-inflammatory effects.[27–30] Moreover, it has been reported that adiponectin reduces the attachment of monocytes to the endothelium by down-regulating the expression of vascular cell adhesion molecule–1, intercellular adhesion molecule-1, and E-selectin[27] and that it inhibits phagocytic activity and production of TNF-α and IL-6 from cultured macrophages.[31] These results indicate that HGF, VEGF, and adiponectin play a crucial role in intestinal mucosal wound healing. In the present study, significant amounts of HGF, VEGF, and adiponectin were detected in the culture supernatants of ADSCs (Fig. 6), indicating that ADSCs injected into the submucosa may secrete these cytokines in situ, resulting in the acceleration of regeneration of wound mucosa and also inhibition of the inflammation observed in TNBS-induced colitis. This possibility was actually confirmed by the in vivo examination in which

FIGURE 10. Distribution of ADSCs in vivo by FISH. A: Fluorescence microscopy of colon 8 days after submucosal injection of 10^7 ADSCs (×10) showing almost healed to normal mucosa. B: Ulcer area undergoing healing. C–E: Distribution of ADSCs or ADSC-derived cells (Y-chromosome-positive cells) in mucosal (C), submucosal (D), and muscular layer (E). F: Y-chromosome-positive cells were counted in 3 low-magnification fields per rat colon 8 days after submucosal injection of ADSCs. Columns and bars represent the means ± SDs of 10 rats ($^*P < 0.001$).

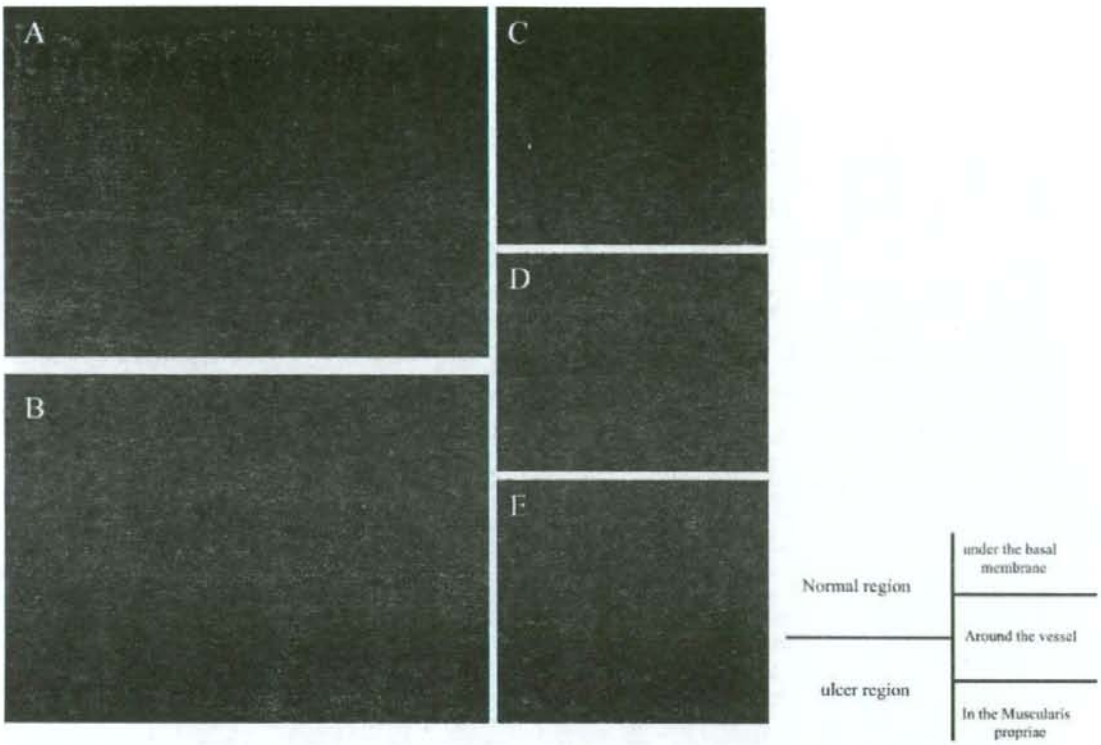
A
B
C
D
E
Normal region
ulcer region
under the basal membrane
Around the vessel
In the Muscularis propriae

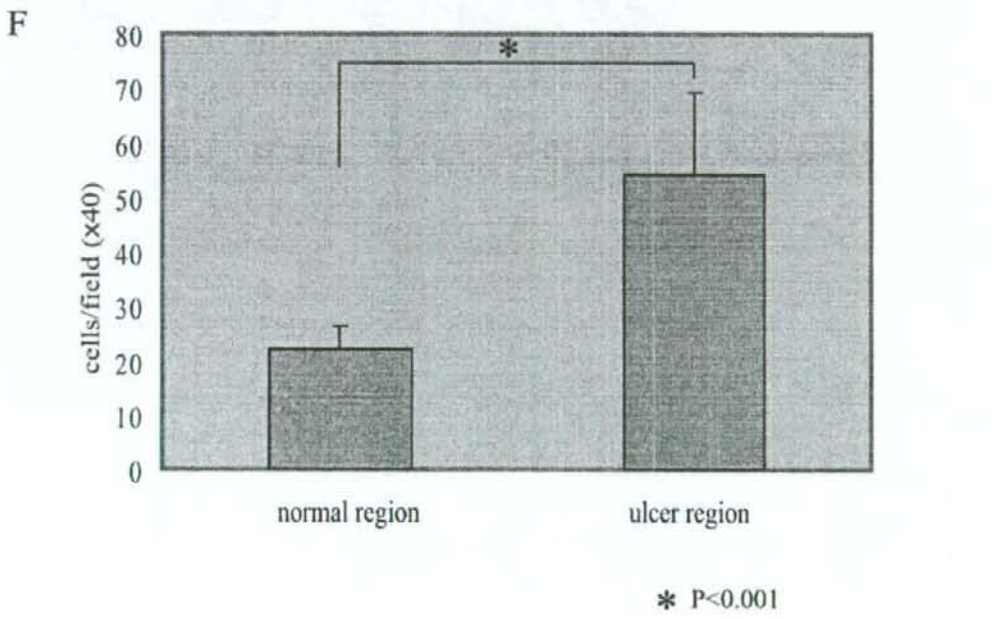
F
cells/field (x40)
80
70
60
50
40
30
20
10
0
*
normal region
ulcer region
* P<0.001

835

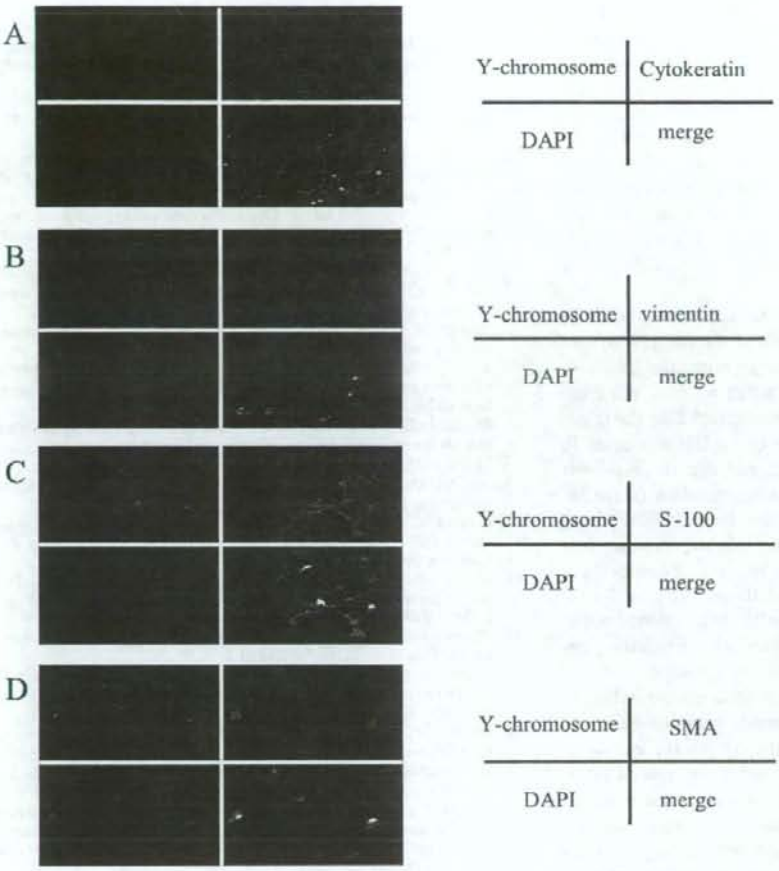

FIGURE 11. Immunofluorescent staining of Y-chromosome-positive cells. A: Y-chromosome-positive cells were not detected in epithelial cells that were stained by cytokeratin. B: Y-chromosome-positive cells were detected in fibroblast-like cells that were stained by vimentin. C: Y-chromosome-positive cells were detected in adipose tissues that were stained by S-100. D: Y-chromosome-positive cells were detected in the muscularis propria layer stained by SMA.

ADSCs facilitated the repair of colonic ulcers (Fig. 8) and reduced inflammatory responses along with TNBS-induced colitis (Fig. 9). There was no statistically significant differences in colon length between the group submucosally injected with ADSCs and the group injected with PBS. This might have been a result of the large ulcer being detected in a limited area of colon in TNBS-induced colitis-model rats in contrast to pan-colitis-model rats.

However, the decreases in the levels of IL-8 in the colonic tissue after the injection of ADSCs clearly indicate the wound-healing effects of ADSCs (Fig. 9), as also shown in the analyses of colon weight as an index of edema (Fig. 7). Furthermore, it is noted that the reduced activity of MPO observed in the colonic tissue confirms decreased infiltration of neutrophils and strengthens the effect of ADSCs. From these findings, it can be speculated that ADSCs prevent both the accumulation and the activation of neutrophils, thereby attenuating the neutrophil-dominant inflammation in colonic tissue caused by TNBS through the reduction of IL-8 levels that play a pivotal role in the accumulation of circulating leukocytes in inflammatory foci.[32] Furthermore, the effect of ADSCs might also be attributable to the anti-inflammatory effect of adiponectin, as shown in the previous study, in which adiponectin was found to exert its anti-inflammatory effect by inhibiting IL-8 production.[30] In addition, adiponectin promotes angiogenesis in response to tissue ischemia.[33] These data suggest that adiponectin secreted by ADSCs may also play a crucial role in TNBS-induced colitis.

As shown in Figure 10, cells derived from ADSCs, defined by Y-FISH, were detected in the mucosal layer under the basal membrane, the submucosal layer around the vessel, and the muscle layer; they were especially observed in the area of inflammation, such as the ulcer edge. They could be thought to differentiate into fibroblast-lineage (vimentin-positive cells), adipocyte-lineage (S-100-positive cells), and muscle-lineage cells (SMA-positive cells) when immunohis-

tochemically examined. However, they were not detected in the epithelial layer, indicating that ADSCs (submucosally injected) did not differentiate into epithelial-lineage or neural-lineage cells, even though they differentiated into various lineage cells in vitro (Figs. 4 and 5). This is in contrast with the findings that bone marrow MSCs were detected in the epithelium of the stomach and intestine[34] and differentiated into neural cells[35] and that MSCs in bone marrow seem to be more primitive than ADSCs. Therefore, our results indicate that although ADSCs have the potential to differentiate into various lineage cells in vitro, ADSCs in vivo can differentiate into mesodermal lineage cells.

Examination in vitro showed that collectively, ADSCs have multiple differentiation ability and secrete growth factors such as VEGF and HGF in large quantities and also produce adiponectin. Therefore, although we have not measured the tissue levels of these growth factors after the injection of ADSCs, it is highly feasible that ADSCs injected in vivo (1×10^7 cells) produce them and that these soluble factors might be responsible for the regeneration of the injured regions observed in the TNBS-induced colitis. Moreover, some ADSCs may differentiate into the various components of the colon, such as smooth muscles, fibroblasts, and myofibroblasts. These mesodermal cells are essential for facilitating the regeneration of epithelial cells. Furthermore, ADSCs improved TNBS-induced colitis by ameliorating colonic injury induced by proinflammatory cytokines.

Importantly, the safety of high-dose lipoaspiration to obtain ADSCs in humans was already established,[36] and thus ADSCs are a viable therapeutic option for amelioration of Crohn's disease or IBD by repairing injured intestinal mucosa. If the number of ADSCs obtained from the subcutaneous adipose tissues of the abdomens of patients themselves is enough to use for the cell therapy, ADSCs can be immediately applicable without cell culture, and the remaining ADSCs can be kept by cryopreservation for future use when a fistula recurs. In addition, treatment via endoscopy is considered a general and established method, thereby submucosally injecting ADSCs without an operation. It is feasible that in vitro cultured ADSCs inoculated into the submucosa are transformed into tumors. Therefore, we have to examine this possibility for a long life span after the treatment, and these types of experiments are now under investigation.

In conclusion, ADSCs can accelerate the regeneration of injured regions, and HGF, VEGF, and adiponectin produced by ADSCs might be responsible for the regeneration.

ACKNOWLEDGMENTS

The authors thank Mr. Hilary Eastwick-Field, Mr. Brian O'Flaherty, and Ms. K. Ando for their help in the preparation of the manuscript.

REFERENCES

1. Katz AJ, Tholpady A, Tholpady SS, et al. Cell surface and transcriptional characterization of human adipose-derived adherent stromal (hADAS) cells. *Stem Cells.* 2005;23:412–423.
2. Strem BM, Hicok KC, Zhu M, et al. Multipotential differentiation of adipose tissue-derived stem cells [review]. *Keio J Med.* 2005;54:132–141.
3. De Ugarte DA, Morizono K, Elbarbary AS, et al. Comparison of multi-lineage cells from human adipose tissue and bone marrow. *Cells Tissues Organs.* 2004;174:101–109.
4. Lee RH, Kim B, Choi I, et al. Characterization and expression analysis of mesenchymal stem cells from human bone marrow and adipose tissue. *Cell Physiol Biochem.* 2004;14:311–324.
5. Garcia-Olmo D, Garcia-Arranz M, Herreros D, et al. A phase I clinical trial of the treatment of Crohn's fistula by adipose mesenchymal stem cell transplantation. *Dis Colon Rectum.* 2005;48:1416–1423.
6. Schrepfer S, Deuse T, Reichenspurner H, et al. Stem cell transplantation: the lung barrier. *Transplant Proc.* 2007;39:573–576.
7. Kern S, Eichler H, Stoeve J, et al. Comparative analysis of mesenchymal stem cells from bone marrow, umbilical cord blood, or adipose tissue. *Stem Cells.* 2006;24:1294–1301.
8. Woodbury D, Schwarz EJ, Prockop DJ, et al. Adult rat and human bone marrow stromal cells differentiate into neurons. *J Neurosci Res.* 2000; 61:364–370.
9. Zuk PA, Zhu M, Ashjian P, et al. Human adipose tissue is a source of multipotent stem cells. *Mol Biol Cell.* 2002;13:4279–4295.
10. Brzoska M, Geiger H, Gauer S, Baer P. Epithelial differentiation of human adipose tissue-derived adult stem cells. *Biochem Biophys Res Commun.* 2005;330:142–150.
11. Morris GP, Beck PL, Herridge MS, et al. Hapten-induced model of chronic inflammation and ulceration in the rat colon. *Gastroenterology.* 1989;96:795–803.
12. Macpherson BR, Pfeiffer CJ. Experimental production of diffuse colitis in rats. *Digestion.* 1978;17:135–150.
13. Tsune I, Ikejima K, Hirose M, et al. Dietary glycine prevents chemical-induced experimental colitis in the rat. *Gastroenterology.* 2003;125: 775–785.
14. Krawisz JE, Sharon P, Stenson WF. Quantitative assay for acute intestinal inflammation based on myeloperoxidase activity. Assessment of inflammation in rat and hamster models. *Gastroenterology.* 1984;87: 1344–1350.
15. Javazon EH, Colter DC, Schwarz EJ, et al. Rat marrow stromal cells are more sensitive to plating density and expand more rapidly from single-cell-derived colonies than human marrow stromal cells. *Stem Cells.* 2001;19:219–225.
16. Yoshimura H, Muneta T, Nimura A, et al. Comparison of rat mesenchymal stem cells derived from bone marrow, synovium, periosteum, adipose tissue, and muscle. *Cell Tissue Res.* 2007;327:449–462.
17. Ashjian PH, Elbarbary AS, Edmonds B, et al. In vitro differentiation of human processed lipoaspirate cells into early neural progenitors. *Plast Reconstr Surg.* 2003;111:1922–1931.
18. Brzoska M, Geiger H, Gauer S, et al. Epithelial differentiation of human adipose tissue-derived adult stem cells. *Biochem Biophys Res Commun.* 2005;330:142–150.
19. Gimble JM, Guilak F. Adipose-derived adult stem cells: isolation, characterization, and differentiation potential. *Cytotherapy.* 2003;5:362–369.
20. Rehman J, Traktuev D, Li J, et al. Secretion of angiogenic and antiapoptotic factors by human adipose stromal cells. *Circulation.* 2004; 109:1292–1298.
21. Zvonic S, Lefevre M, Kilroy G, et al. Secretome of primary cultures of human adipose-derived stem cells: modulation of serpins by adipogenesis. *Mol Cell Proteomics.* 2007;6:18–28.
22. Van Belle E, Witzenbichler B, Chen D, Silver et al. Potentiated angiogenic effect of scatter factor/hepatocyte growth factor via induction of vascular endothelial growth factor: the case for paracrine amplification of angiogenesis. *Circulation.* 1998;97:381–390.
23. Yaekashiwa M, Nakayama S, Ohnuma K, et al. Simultaneous or delayed administration of hepatocyte growth factor equally represses the fibrotic changes in murine lung injury induced by bleomycin. A morphologic study. *Am J Respir Crit Care Med.* 1997;156:1937–1944.

24. Matsuda Y, Matsumoto K, Yamada A, et al. Preventive and therapeutic effects in rats of hepatocyte growth factor infusion on liver fibrosis/cirrhosis. *Hepatology.* 1997;26:81–89.
25. Xin X, Yang S, Ingle G, et al. Hepatocyte growth factor enhances vascular endothelial growth factor-induced angiogenesis in vitro and in vivo. Am J Pathol. 2001;158:1111–1120.
26. Numata M, Ido A, Moriuchi A, et al. Hepatocyte growth factor facilitates the repair of large colonic ulcers in 2,4,6-trinitrobenzene sulfonic acid-induced colitis in rats. *Inflamm Bowel Dis.* 2005;11:551–558.
27. Ouchi N, Kihara S, Arita Y, et al. Novel modulator for endothelial adhesion molecules: adipocyte-derived plasma protein adiponectin. *Circulation.* 1999;100:2473–2476.
28. Wulster-Radcliffe MC, Ajuwon KM, Wang J, et al. Adiponectin differentially regulates cytokines in porcine macrophages. *Biochem Biophys Res Commun.* 2004,;316:924–929.
29. Wolf AM, Wolf D, Rumpold H, Enrich B, Tilg H. Adiponectin induces the anti-inflammatory cytokines IL-10 and IL-1RA in human leukocytes. *Biochem Biophys Res Commun.* 2004;323:630–635.
30. Nishihara T, Matsuda M, Araki H, et al. Effect of adiponectin on murine colitis induced by dextran sulfate sodium. *Gastroenterology.* 2006;131:853–861.
31. Yokota T, Oritani K, Takahashi I, et al. Adiponectin, a new member of the family of soluble defense collagens, negatively regulates the growth of myelomonocytic progenitors and the functions of macrophages. *Blood.* 2000;96:1723–1732.
32. Pender SL, Chance V, Whiting CV, et al. Systemic administration of the chemokine macrophage inflammatory protein 1alpha exacerbates inflammatory bowel disease in a mouse model. *Gut.* 2005;54:1114–1120.
33. Shibata R, Ouchi N, Kihara S, et al. Adiponectin stimulates angiogenesis in response to tissue ischemia through stimulation of amp-activated protein kinase signaling. *J Biol Chem.* 2004;279:28670–28674.
34. Semont A, Francois S, Mouiseddine M, et al. Mesenchymal stem cells increase self-renewal of small intestinal epithelium and accelerate structural recovery after radiation injury. *Adv Exp Med Biol.* 2006;585:19–30.
35. Sanchez-Ramos J, Song S, Cardozo-Pelaez F, et al. Adult bone marrow stromal cells differentiate into neural cells in vitro. *Exp Neurol.* 2002;164:247–256.
36. Cardenas-Camarena L. Lipoaspiration and its complications: a safe operation. *Plast Reconstr Surg.* 2003;112:1435–1441; discussion 1442–1443.

MyD88-Dependent Pathway in T Cells Directly Modulates the Expansion of Colitogenic CD4$^+$ T Cells in Chronic Colitis[1]

Takayuki Tomita,* Takanori Kanai,[2]* Toshimitsu Fujii,* Yasuhiro Nemoto,* Ryuichi Okamoto,* Kiichiro Tsuchiya,* Teruji Totsuka,* Naoya Sakamoto,* Shizuo Akira,† and Mamoru Watanabe*

TLRs that mediate the recognition of pathogen-associated molecular patterns are widely expressed on/in cells of the innate immune system. However, recent findings demonstrate that certain TLRs are also expressed in conventional TCR$\alpha\beta^+$ T cells that are critically involved in the acquired immune system, suggesting that TLR ligands can directly modulate T cell function in addition to various innate immune cells. In this study, we report that in a murine model of chronic colitis induced in RAG-2$^{-/-}$ mice by adoptive transfer of CD4$^+$CD45RB^{high} T cells, both CD4$^+$CD45RB^{high} donor cells and the expanding colitogenic lamina propria CD4$^+$CD44^{high} memory cells expresses a wide variety of TLRs along with MyD88, a key adaptor molecule required for signal transduction through TLRs. Although RAG-2$^{-/-}$ mice transferred with MyD88$^{-/-}$CD4$^+$CD45RB^{high} cells developed colitis, the severity was reduced with the delayed kinetics of clinical course, and the expansion of colitogenic CD4$^+$ T cells was significantly impaired as compared with control mice transferred with MyD88$^{+/+}$CD4$^+$CD45RB^{high} cells. When RAG-2$^{-/-}$ mice were transferred with the same number of MyD88$^{+/+}$ (Ly5.1$^+$) and MyD88$^{-/-}$ (Ly5.2$^+$) CD4$^+$CD45RB^{high} cells, MyD88$^{-/-}$CD4$^+$ T cells showed significantly lower proliferative responses assessed by in vivo CFSE division assay, and also lower expression of antiapoptotic Bcl-2/Bcl-x$_L$ molecules and less production of IFN-γ and IL-17, compared with the paired MyD88$^{+/+}$CD4$^+$ T cells. Collectively, the MyD88-dependent pathway that controls TLR signaling in T cells may directly promote the proliferation and survival of colitogenic CD4$^+$ T cells to sustain chronic colitis. *The Journal of Immunology*, **2008, 180: 5291–5299.**

Inflammatory bowel diseases (IBD)[3] are caused by excessive tissue damaging by chronic inflammatory responses in the gut wall, and commonly take persistent courses (1, 2). According to the present understanding, the diseases are caused by infiltrated colitogenic effector/memory CD4$^+$ T cells within the inflamed mucosa, which are presumably primed by commensal Ag-loading dendritic cells (DCs) in lymphoid tissues (3). However, the nature of colitogenic CD4$^+$ T cells over time during chronic colitis under the persistent presence of commensal bacteria remains largely unknown.

Importantly, it is well-known that experimental colitis does not develop when mice are kept in a germfree condition (4–6), suggesting that intestinal microflora are essential to initiate and maintain colitogenic CD4$^+$ T cells by stimuli through 1) TCR signaling by one or more commensal Ags (signal 1) and 2) TLR signaling by pathogen-associated molecular patterns (PAMPs) in addition to cytokines (signal 3) and costimulatory signaling (signal 2) (7, 8). However, there are no reports showing that TLR signaling directly stimulates colitogenic CD4$^+$ T cells for their proliferation and/or survival.

It is widely recognized that TLRs are expressed in/on the innate immune cells (9, 10), such as macrophages, DCs, and epithelial cells, and are crucially important primarily to activate these professional and nonprofessional APCs and secondarily promote T cell responses (11). However, accumulating evidence has shown that certain TLRs are also expressed on/in TCR$\alpha\beta^+$ T cells that are major acquired immune cell populations (12), suggesting that TLR signaling may possibly have some direct function on adaptive immunity. Hence, to assess the direct role of TLR signaling initiated by PAMPs of commensal bacteria in modulation of colitogenic CD4$^+$ T cell expansion during the development and the persistence of chronic colitis, we performed a series of adoptive transfer colitis experiments by transfer of CD4$^+$CD45RB^{high} T cells that are deficient for MyD88, a key adaptor molecule of TLR signaling (13, 14), into RAG-2$^{-/-}$ recipient mice whose TLR pathways remained intact throughout the innate immune system.

Materials and Methods

Animals

Six- to 10-wk-old Ly5.2-background (Ly5.2$^+$) MyD88$^{-/-}$ mice (13) were used. Ly5.2$^+$ C57BL/6 mice were purchased from Japan Clea. Ly5.1-background C57BL/6 mice and Ly5.2$^+$ C57BL/6 RAG-2$^{-/-}$ mice were obtained from Taconic Farms and Central Laboratories for Experimental Animals (Kawasaki, Japan). Mice were maintained under specific pathogen-free conditions in the Animal Care Facility of Tokyo Medical and Dental University (Tokyo, Japan). All experiments were approved by the

*Department of Gastroenterology and Hepatology, Graduate School, Tokyo Medical and Dental University, Tokyo, Japan; and †Department of Host Defense, Research Institute for Microbial Diseases, Osaka University, Osaka, Japan

Received for publication July 26, 2007. Accepted for publication February 16, 2008.

The costs of publication of this article were defrayed in part by the payment of page charges. This article must therefore be hereby marked *advertisement* in accordance with 18 U.S.C. Section 1734 solely to indicate this fact.

[1] This work was supported in part by Grants-in-Aid for Scientific Research, Scientific Research on Priority Areas, Exploratory Research and Creative Scientific Research from the Japanese Ministry of Education, Culture, Sports, Science, and Technology; the Japanese Ministry of Health, Labor, and Welfare; the Japan Medical Association; and Foundation for Advancement of International Science.

[2] Address correspondence and reprint requests to Dr. Takanori Kanai, Department of Gastroenterology and Hepatology, Graduate School, Tokyo Medical and Dental University, 1-5-45 Yushima, Bunkyo-ku, Tokyo 113-8519, Japan. E-mail address: taka.gast@tmd.ac.jp

[3] Abbreviations used in this paper: IBD, inflammatory bowel disease; DC, dendritic cell; PAMP, pathogen-associated molecular pattern; PB, peripheral blood; SP, spleen; MLN, mesenteric lymph node; BM, bone marrow; WT, wild type; LP, lamina propria; IEL, intraepithelial cell; HPF, high-power field.

regional animal study committees and were done according to institutional guidelines and Home Office regulations.

Purification of T cell subsets

For isolation of peripheral blood (PB) lymphocytes, 600 μl of PB was collected from each mouse and was diluted 1/1 with PBS. The diluted PB was layered over Lymphosepar II (IBL) and centrifuged at 400 × *g* for 30 min at room temperature. Lymphocytes were then isolated from the plasma-Ficoll interface. Spleen (SP) and mesenteric lymph nodes (MLN) were mechanically disrupted into single-cell suspensions. Bone marrow (BM) was collected from the femur by flushing with sterile PBS.

$CD4^+$ T cells were isolated from SP cells of $MyD88^{-/-}$ and littermate $MyD88^{+/+}$ mice using the anti-CD4 (L3T4)-MACS system (Miltenyi Biotec) according to the manufacturer's instruction. Enriched $CD4^+$ T cells (94–96% pure, as estimated by FACSCalibur; BD Biosciences) were then labeled with PE-conjugated anti-mouse CD4 (RM4-5; BD Pharmingen) and FITC-conjugated anti-CD45RB (16A; BD Pharmingen). The subpopulation of $CD4^+CD45RB^{high}$ cells was collected by two-color sorting on a FACS Aria (BD Biosciences), and was >98.0% pure on reanalysis.

To obtain LP $CD4^+$ T cells, colitis was induced in $RAG\text{-}2^{-/-}$ mice by adoptive transfer of $CD4^+CD45RB^{high}$ T cells either from $MyD88^{-/-}$ or from littermate wild-type (WT) $MyD88^{+/+}$ mice as described previously (15). Colitic $CD4^+CD45RB^{high}$ T cell-transferred $RAG\text{-}2^{-/-}$ mice were sacrificed at 6–10 wk after transfer. The entire colon was opened longitudinally, washed with PBS, and cut into small pieces. The dissected mucosa was incubated with Ca^{2+}, Mg^{2+}-free HBSS containing 1 mM DTT (Sigma-Aldrich) for 45 min to remove mucus and then treated with 2.0 mg/ml collagenase (Roche) and 0.01% DNase (Worthington Biomedical) for 2 h. The cells were pelleted twice through a 40% isotonic Percoll solution, and then subjected to Ficoll-Hypaque density gradient centrifugation (40%/75%). Enriched lamina propria (LP) $CD4^+$ T cells were obtained by positive selection using anti-CD4 (L3T4) MACS magnetic beads. The resultant cells contained >95% $CD4^+$ cells when analyzed by FACSCalibur. To assess the expression of TLRs and MyD88 in $CD4^+$ T cells using RT-PCR, every cell population was isolated by FACS Aria (BD Biosciences) to gain >98% $CD4^+$ purity.

RT-PCR

Total RNA was isolated by using Isogen reagent (Nippon Gene). Aliquots of total RNA (0.5 μg) were used for cDNA synthesis in a 20-μl reaction volume using random primers. One microliter of reverse transcription product was amplified with 0.25 U of rTaq DNA polymerase (Toyobo) in a 25-μl reaction. Sense and antisense primers and the cycle numbers for the amplification of each gene (16) were as follows: TLR1, sense 5′-TCTCT GAAGGCTTTGTCGATACA-3′ and antisense 5′-GACAGAGCCTGTA AGCATATTCG-3′ (35 cycles); TLR2, sense 5′-TCTAAAGTCGATC CGCGACAT-3′ and antisense 5′-TACCCAGCTCGCTCACTACGT-3′ (35 cycles); TLR3, sense 5′-TTGTCTTCTGCACGAACCTG-3′ and antisense 5′-CGCAACGCAAGGATTTTATT-3′ (35 cycles); TLR4, sense 5′-CAAGAACATAGATCTGAGCTTCAACCC-3′ and antisense 5′-GCT GTCCAATAGGGAAGCTTTCTAGAG-3′ (35 cycles); TLR5, sense 5′-ACTGAATTCCTTAAGCGACGTA-3′ and antisense 5′-AGAAGATAA AGCCGTGCGAAA-3′ (35 cycles); TLR6, sense 5′-AACAGGATAC GGAGCCTTGA-3′ and antisense 5′-CCAGGAAAGTCAGCTTCGTC-3′ (35 cycles); TLR7, sense 5′-TTCCGATACGATGAATATGCACG-3′ and antisense 5′-TGAGTTTGTCCAGAAGCCGTAAT-3′ (35 cycles); TLR8, sense 5′-GGCACAACTCCCTTGTGATT-3′ and antisense 5′-CATTTG GGTGCTGTTGTTTG-3′ (35 cycles); TLR9, sense 5′-CCGCAAGA CTCTATTTGTGCTGG-3′ and antisense 5′-TGTCCCTAGTCAGG GCTGTACTCAG-3′ (35 cycles); MyD88, sense 5′-GGCCTTGTTAGA CCGTGAGG-3′ and antisense 5′-TCATCTTCCCCTCTGCCCTA-3′ for (35 cycles); β-actin, sense 5′-GTGGGCCGCTCTAGGCACCAA-3′ and antisense 5′-CTCTTTGATGTCACGCACGATTTC-3′ (30 cycles). PCR products were separated on 1.8% agarose gels, stained with ethidium bromide, and visualized with a Lumi-Imager F1 (Roche Diagnostics).

Quantitative PCR

To validate gene expression changes, quantitative RT-PCR analysis was performed by Applied Biosystems 7500 using validated TaqMan Gene Expression Assays (Applied Biosystems). The TaqMan probes and primers for mouse Bcl-2 (assay identification number Mm00477631_m1) and mouse Bcl-x_L (assay identification number Mm00437783_m1) were Assay-on-Demand gene expression products (Applied Biosystems). The mouse β-actin gene was used as endogenous control (catalog number 4352933E; Applied Biosystems). The thermal cycler conditions were as follows: hold for 10 min at 95°C, followed a cycle of 95°C for 15 s and 60°C for 1 min for 45 cycles. All samples were performed in triplicate.

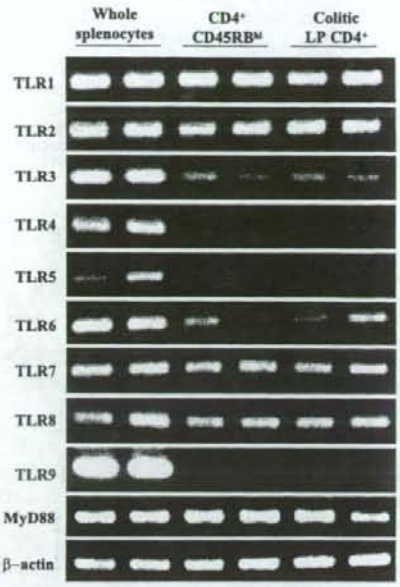

FIGURE 1. $CD4^+CD45RB^{high}$ donor cells and colitic LP $CD4^+$ T cells express mRNAs for TLR and MyD88. Splenocytes and $CD4^+CD45RB^{high}$ T cells from normal C57BL/6 mice, or LP $CD4^+$ T cells from colitic $RAG\text{-}2^{-/-}$ mice transferred with $CD4^+CD45RB^{high}$ T cells, were strictly isolated using FACSAria (purity, >98.0%) and subjected for total RNA extraction. The RNA was reverse transcripted and amplified with gene for specific primers. PCR products were separated by agarose gel electrophoresis and stained with ethidium bromide. All the RT-PCR experiments were performed at least three times on independent samples.

Amplification data were analyzed with an Applied Biosystems Sequence Detection Software version 1.3. The relative expression of the gene of interest was normalized by the expression of β-actin.

In vivo experimental design

We performed a series of in vivo transfer experiments to investigate the role of TLR signaling in $CD4^+CD45RB^{high}$ T cells or in colitogenic LP $CD4^+$ T cells in the development and persistence of murine chronic colitis.

Experiment 1. To assess the requirement of MyD88-dependent signaling in the development of colitis including the processes for T cell priming and activation, along with the persistence of colitogenic effector or memory $CD4^+$ T cells, we performed a cell transfer experiment using $MyD88^{-/-}$ and littermate WT $MyD88^{+/+}$ mice as donors. $CD4^+CD45RB^{high}$ T cells from $MyD88^{-/-}$ ($n = 6$) or $MyD88^{+/+}$ ($n = 6$) donors were injected i.p. into $RAG\text{-}2^{-/-}$ mice and the recipients were monitored for 4–6 wk after transfer. In another set of experiment using the present protocol, we monitored the groups of mice (each $n = 5$) to 10 wk after transfer to assess the kinetics of the development.

Experiment 2. To further assess the necessity of MyD88-dependent signaling in the development of colitis, we performed in vivo competition experiments. The same number (2.5×10^5 cells/mouse) of $CD4^+CD45RB^{high}$ T cells from $MyD88^{+/+}$ ($Ly5.1^+$) or $MyD88^{-/-}$ ($Ly5.2^+$) mice were coinjected i.p. into $RAG\text{-}2^{-/-}$ mice ($n = 6$), and the recipients were monitored for 6 wk after transfer.

Experiment 3. To assess the requirement of MyD88-dependent signaling for the persistence of colitogenic memory $CD4^+$ T cells in this $CD4^+CD45RB^{high}$ T cell-transferred colitis model, independently from the impact of naive T cell priming, activation, and differentiation, we performed the adoptive retransfer of colitogenic LP memory $CD4^+$ T cells derived from colitic mice that were transferred with $CD4^+CD45RB^{high}$ T cells of either $MyD88^{+/+}$ ($n = 6$) or $MyD88^{-/-}$ mice ($n = 6$) after 10 wk from transfer (17).

Experiment 4. To further assess the requirement of MyD88-dependent signaling for the persistence of colitogenic memory $CD4^+$ T cells, we

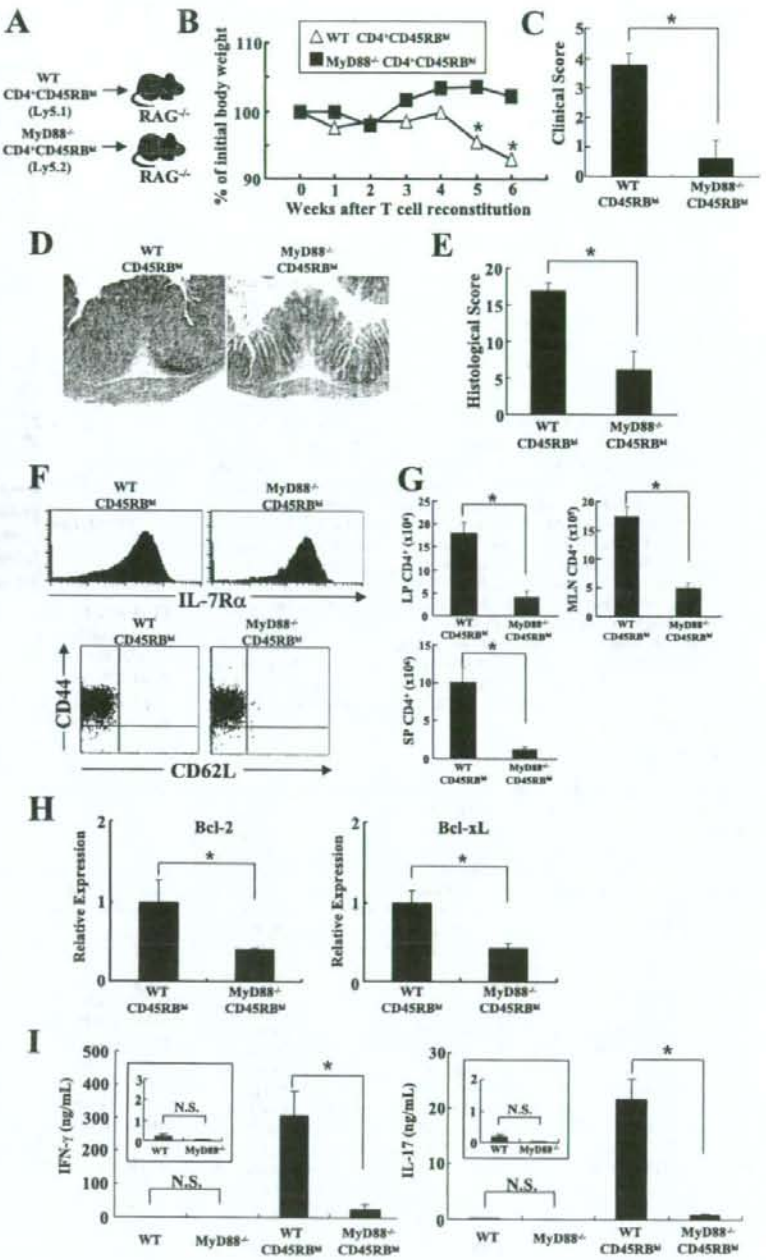

FIGURE 2. RAG-$2^{-/-}$ mice transferred with MyD88$^{-/-}$CD4$^+$CD45RB^{high} T cells develop milder colitis. *A*, RAG-$2^{-/-}$ mice were transferred with splenic MyD88$^{+/+}$ (WT) ($n = 6$) or MyD88$^{-/-}$ ($n = 6$) CD4$^+$CD45RB^{high} T cells (3×10^5 cells/mouse). *B*, Change in body weight over time is expressed as percent of the original weight. Data are represented as the mean ± SEM of six mice in each group. *, $p < 0.05$. *C*, Clinical scores were determined at 6 wk after transfer as described in *Materials and Methods*. Data are indicated as mean ± SEM of six mice in each group. *, $p < 0.01$. *D*, Histological examination of the colon from WT (*left*) or MyD88$^{-/-}$ (*right*) CD4$^+$CD45RB^{high} T cells at 6 wk after transfer. Original magnification, ×100. *E*, Histological scoring of mice transferred with WT or MyD88$^{-/-}$CD4$^+$CD45RB^{high} T cells at 6 wk after transfer. Data are indicated as mean ± SEM of six mice in each group. *, $p < 0.01$. *F*, Phenotypic characterization of LP CD4$^+$ T cells isolated from mice transferred with WT or MyD88$^{-/-}$CD4$^+$CD45RB^{high} T cells at 6 wk after transfer. *G*, LP, MLN, and SP CD4$^+$ T cells were isolated from mice transferred with WT or MyD88$^{-/-}$CD4$^+$CD45RB^{high} T cells at 6 wk after transfer, and the number of CD4$^+$ cells was determined by flow cytometry. Data are indicated as mean ± SEM of six mice in each group. *, $p < 0.01$. *H*, Expression of Bcl-2 and Bcl-x_L mRNAs in SP cells was determined by quantitative RT-PCR, and are shown as relative amount of indicated mRNA normalized by expression of β-actin. Data are represented as the mean ± SEM of six samples. *, $p < 0.05$. *I*, Cytokine production by LP CD4$^+$ T cells. LP CD4$^+$ T cells were isolated at 6 wk after transfer and stimulated with anti-CD3 and anti-CD28 mAbs for 48 h. IFN-γ and IL-17 concentrations in culture supernatants were measured by ELISA. Data are indicated as mean ± SEM of six mice in each group. *, $p < 0.01$. WT; healthy WT mice, MyD88$^{-/-}$; healthy MyD88$^{-/-}$ mice, WT CD45RB^{high}; RAG-$2^{-/-}$ mice transferred with WT CD4$^+$CD45RB^{high} T cells, MyD88$^{-/-}$CD45RB^{high}; RAG-$2^{-/-}$ mice transferred with MyD88$^{-/-}$CD4$^+$ CD45RB^{high} T cells.

performed in vivo competition experiments. The same number (2.0×10^5 cells/mouse) of colitogenic LP memory CD4$^+$ T cells obtained from colitic mice that were transferred with either MyD88$^{+/+}$ (Ly5.1$^+$) or MyD88$^{-/-}$ (Ly5.2$^+$) CD4$^+$CD45RB^{high} T cells from either MyD88$^{+/+}$ mice (Ly5.1$^+$) or MyD88$^{-/-}$ mice (Ly5.2$^+$) after 10 wk from transfer were coinjected i.p. into new RAG-$2^{-/-}$ mice ($n = 6$), and the mice were monitored for 6 wk after the retransfer.

In experiments 1–4, all mice were assessed for a clinical score (18) that is the sum of four parameters listed as follows: hunching and wasting, 0 or 1; colon thickening, 0–3 (0, no colon thickening; 1, mild thickening; 2, moderate thickening; 3, extensive thickening); and stool consistency, 0–3 (0, normal beaded stool; 1, soft stool; 2, diarrhea; 3, bloody stool) (18). To monitor the clinical sign during the observed period over time, the ongoing disease activity index is defined as the sum (0–5 points) of the above-mentioned parameters except the colon thickening.

Experiment 5. To assess the requirement of MyD88-dependent signaling for the lymphopenia-driven rapid proliferation (19) of colitogenic memory CD4$^+$ T cells, we performed a short-term observation of in vivo competition experiments in combination with the CFSE-labeling method. The same number (2.0×10^6 cells/mouse) of CFSE-labeled LP memory CD4$^+$ T cells from colitic mice that were initially transferred with MyD88$^{+/+}$ (Ly5.1$^+$) or MyD88$^{-/-}$ (Ly5.2$^+$) CD4$^+$CD45RB^{high} T cells at 10 wk after transfer were injected i.p. into new RAG-$2^{-/-}$ mice ($n = 6$). In experiment 5, mice were sacrificed 10 days after retransfer, and assessed for cell divisions by CFSE dilution.

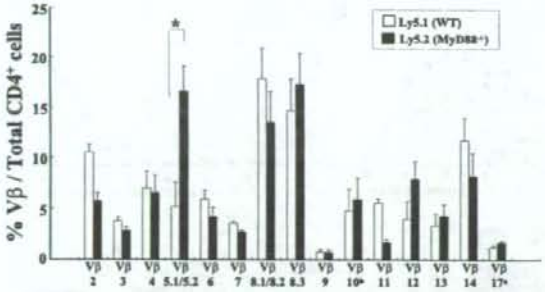

FIGURE 3. Vβ repertoire shows little difference between MyD88$^{+/+}$ or MyD88$^{-/-}$ donor cells. To analyze the TCR Vβ family repertoire, SP cells were isolated from mice transferred with Ly5.1$^+$MyD88$^{+/+}$ (WT) or Ly5.2$^+$MyD88$^{-/-}$CD4$^+$CD45RB^{high} T cells at 6 wk after transfer, and then triple-stained with PerCP-conjugated ant-CD3ε mAb (145-2C11), PE-conjugated anti-CD4 mAb (RM4-5), and a panel of 15 FITC-conjugated Vβ mAbs. Each percentage value indicates the frequency of each Vβ pooled from three independent experiments ($n = 6$). *, $p < 0.05$.

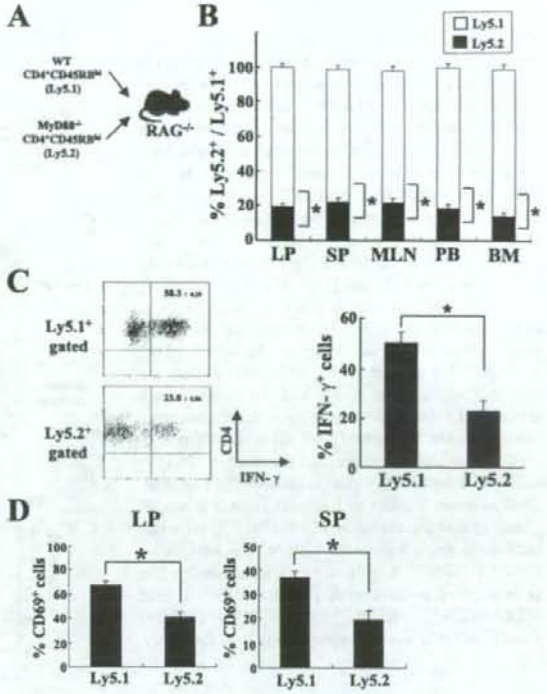

FIGURE 4. Expansive activity of MyD88$^{+/+}$ donor cells predominates over that of MyD88$^{-/-}$ donor cells in an in vivo competition assay. *A*, The same number (2.5×10^5 cells/mouse) of CD4$^+$CD45RB^{high} T cells from Ly5.1$^+$MyD88$^{+/+}$ (WT) mice and Ly5.2$^+$MyD88$^{-/-}$ mice was coinjected i.p. into RAG-2$^{-/-}$ mice ($n = 6$). *B*, Six weeks after transfer, LP, SP, MLN, PB, and BM CD4$^+$ T cells were isolated, and the ratio of Ly5.1$^+$ and Ly5.2$^+$ CD4$^+$ cells was determined by flow cytometry. *, $p < 0.01$. *C*, The frequencies of IFN-γ-producing LP CD4$^+$ T cells per total Ly5.1$^+$ or Ly5.2$^+$ cells were analyzed in the indicated subpopulations by flow cytometry. Data are represented as mean ± SEM of three independent experiments. *, $p < 0.01$. *D*, Phenotypic characterization of LP and SP CD4$^+$ T cells after transfer of CD4$^+$CD45RB^{high} T cells. % CD69$^+$, Percentages of CD4$^+$CD69$^+$ cells per total CD4$^+$ cells. Data are represented as mean ± SEM of six mice per group. *, $p < 0.05$.

Histological examination

Tissue samples were fixed by 10% neutral-buffered formalin, and paraffin-embedded sections (5 μm) were stained with H&E. Three tissue samples from the proximal, middle, and distal parts of the colon were prepared and subjected for analysis. The sections were analyzed without prior knowledge of the type of T cell reconstitution. The most affected area was graded by the severity of lesions. The degree of colonic inflammation was calculated using a previous scoring system (20): mucosa damage, 0; normal, 1; 3–10 intraepithelial cells (IEL)/high power field (HPF) and focal damage, 2; >10 IEL/HPF and rare crypt abscesses, 3; >10 IEL/HPF, multiple crypt abscesses and erosion/ulceration, submucosa damage, 0; normal or widely scattered leukocytes, 1; focal aggregates of leukocytes, 2; diffuse leukocyte infiltration with expansion of submucosa, 3; diffuse leukocyte infiltration, muscularis damage, 0; normal or widely scattered leukocytes, 1; widely scattered leukocyte aggregates between muscle layers, 2; leukocyte infiltration with focal effacement of the muscularis, 3; extensive leukocyte infiltration with transmural effacement of the muscularis.

Cytokine ELISA

To measure cytokine production, 1×10^5 LP CD4$^+$ T cells were cultured in 200 μl of culture medium at 37°C in a humidified atmosphere containing 5% CO_2, using 96-well plates (Costar) which were precoated with 5 μg/ml hamster anti-mouse CD3ε mAb (145-2C11; BD Pharmingen) and hamster 2 μg/ml anti-mouse CD28 mAb (37.51; BD Pharmingen) in PBS overnight at 4°C. Culture supernatants were removed after 48 h and assayed for cytokine production. Cytokine concentrations were determined by specific ELISA following the manufacturer's recommendation (R&D Systems).

Flow cytometry

To detect the surface expression of molecules, isolated splenocytes, MLN, PB, BM, or LP mononuclear cells were preincubated with an FcγR-blocking mAb (CD16/32; 2.4G2; BD Pharmingen) for 15 min followed by incubation with specific FITC-, PE-, PerCP-, allophycocyanin- or biotin-labeled Abs for 20 min on ice. The following mAbs except biotin-conjugated anti-mouse IL-7Rα (A7R34; eBioscience) were obtained from BD Pharmingen; anti-CD3ε mAb (145-2C11), anti-CD4 mAb (RM4-5), anti-CD45RB mAb (16A), anti-CD62L (MEL-14), anti-CD44 mAb (IM7), anti-CD69 mAb (H1.2F3). Biotinylated Abs were detected with PE-streptavidin. Standard three- or four-color flow cytometric analysis was performed by the FACSCalibur equipped with CellQuest software. Background fluorescence was assessed by the staining of control irrelevant isotype. To analyze the TCR Vβ family repertoire, splenic cells were triple-stained with PerCP-conjugated anti-CD3ε mAb (145C-11), PE-conjugated anti-CD4 mAb (RM4-5), and either of the following FITC-conjugated mAbs: Vβ2; KJ25, Vβ3; KT4, Vβ4; MR9-4, Vβ5.1/5.2; RR4-7, Vβ6; TR310, Vβ7; MR5-2, Vβ8.1/2; B21.14, Vβ8.3; MR10-2, Vβ9; B21.5, Vβ10^b; RR3-15, Vβ11; MR11-1, Vβ12; IN12.3, Vβ13; 14.2, Vβ14; and KJ23, Vβ17*. All the Abs were purchased from BD Pharmingen.

CFSE labeling of T cells

T cell division in vivo was assessed by flow cytometry of CFSE-labeled cells. Isolated LP CD4$^+$ T cells were stained in vitro with the cytoplasmic dye CFSE (Molecular Probes) before reconstitution by incubation for 10 min at 37°C with 5 μM CFSE. The labeling reaction was quenched by washing in ice-cold RPMI 1640 supplemented with 10% FCS.

Statistical analysis

The results are expressed as mean ± SEM. Groups of data were compared by Mann-Whitney *U* test. Differences in data were considered to be statistically significant when $p < 0.05$.

Results

TLRs are expressed in CD4$^+$CD45RB^{high} donor cells and colitic LP CD4$^+$ cells

To assess the direct involvement of TLR signaling in regulating cell function of CD4$^+$ T cells composing chronic colitis under the presence of commensal bacteria, we examined whether mRNAs of TLR1–9 and their adaptor molecule, MyD88, are expressed in donor T cells or the LP CD4$^+$ T cells in colitic RAG-2$^{-/-}$ mice transferred with CD4$^+$CD45RB^{high} T cells. To do so, we isolated

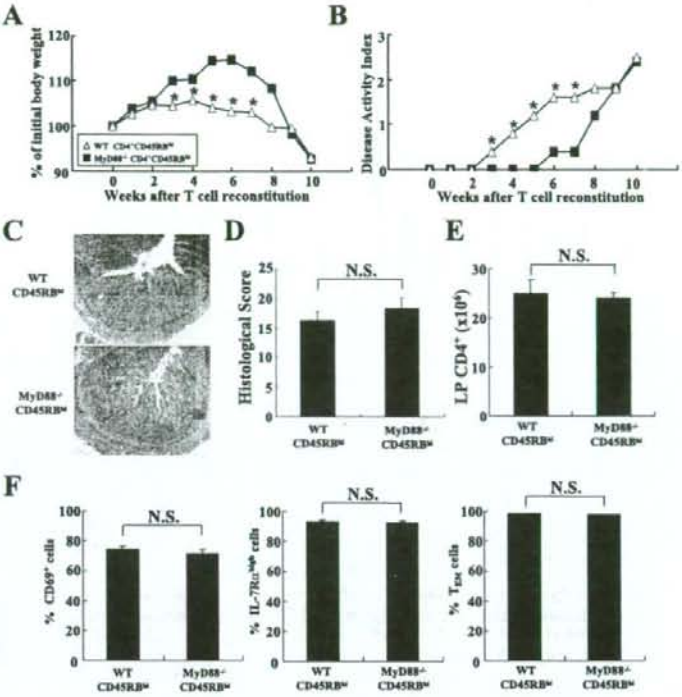

FIGURE 5. RAG-$2^{-/-}$ mice transferred with MyD88$^{-/-}$CD4$^+$CD45RB^{high} T cells develop colitis with the delayed kinetics, but reach to a similar level of mice transferred with MyD88$^{+/+}$CD4$^+$CD45RB^{high} T cells at 10 wk after transfer. *A*, Change in body weight is expressed as the percent of the original weight. Data are represented as mean ± SEM of five mice in each group. *, $p < 0.05$. WT, MyD88$^{+/+}$. *B*, Ongoing disease activity index was monitored during the course. Data are indicated as mean ± SEM of five mice in each group. *, $p < 0.05$. *C*, Histological examination of the colon from WT (*upper*) or MyD88$^{-/-}$ (*lower*) CD4$^+$CD45RB^{high} T cells at 10 wk after transfer. Original magnification, ×100. *D*, Histological scoring of mice transferred with WT or MyD88$^{-/-}$CD4$^+$ CD45RB^{high} T cells at 10 wk after transfer. Data are indicated as the mean ± SEM of five mice in each group. *E*, LP CD4$^+$ T cells were isolated from mice transferred with WT or MyD88$^{-/-}$CD4$^+$CD45RB^{high} T cells at 10 wk after transfer, and the number of CD4$^+$ cells was determined by flow cytometry. Data are indicated as mean ± SEM of five mice in each group. *F*, Phenotypic characterization of LP CD4$^+$ T cells isolated from mice transferred with WT or MyD88$^{-/-}$ CD4$^+$CD45RB^{high} T cells at 10 wk after transfer. The percentage of positive cells per total CD4$^+$ T cells (CD69$^+$/CD4$^+$, IL-7Rα^+/CD4$^+$, CD4$^+$CD44^{high} CD62L$^-$/CD4$^+$) was determined using flow cytometry.

each CD4$^+$ population under highly stringent gate definitions using FACSAria to avoid contamination of cells, such as macrophages, DCs, and B cells. As shown by RT-PCR in Fig. 1, whole splenocytes including T cells, B cells, macrophages, and DCs were used as the positive control, and expressed all members of TLR1–9 and MyD88. Under this condition, CD4$^+$CD45RB^{high} donor cells expressed MyD88 and TLRs except TLR-4, 5, and 9 along with MyD88, while colitic LP CD4$^+$ T cells expressed all members of TLRs and MyD88, indicating that TLR signaling via MyD88 may be directly involved in the priming, activation, proliferation, and survival of CD4$^+$ T cells in the present transfer model. The data were further by completely no detection of PCR products from a template prepared without the addition of reverse transcriptase, excluding a possibility of signals derived from contaminating genomic DNA rather than mRNA (data not shown).

RAG-$2^{-/-}$ mice transferred with MyD88$^{-/-}$ CD4$^+$ CD45RB^{high} T cells developed milder colitis

To explore whether the MyD88-signaling pathway in T cells is involved in the development of chronic colitis, we transferred MyD88$^{-/-}$ or MyD88$^{+/+}$ CD4$^+$CD45RB^{high} T cells into RAG-$2^{-/-}$ (MyD88$^{+/+}$) recipient mice maintaining an intact MyD88-dependent pathway of the innate immune system, meaning that only the transferred CD4$^+$ T cells lack the MyD88-dependent pathway within the recipient mice (Fig. 2*A*). When WT MyD88$^{+/+}$ CD4$^+$CD45RB^{high} cells were transferred into RAG-$2^{-/-}$ mice, the recipients rapidly developed severe wasting disease associated with clinical signs of severe colitis. Particularly, weight loss (Fig. 2*B*), persistent diarrhea and also occasionally bloody stool or anal prolapse was observed by tracking the clinical score up to 6 wk after transfer (Fig. 2*C*). However, when MyD88$^{-/-}$CD4$^+$ CD45RB^{high} T cells were transferred into RAG-$2^{-/-}$ mice, the recipients also developed wasting disease and colitis despite the delayed onset (see the following result in Fig. 5), but the clinical score at 6 wk after transfer was significantly lower as compared with that of mice transferred with control MyD88$^{+/+}$ CD4$^+$CD45RB^{high} T cells (Fig. 2*C*). Thus, the delayed onset and milder clinical score of mice transferred with MyD88$^{-/-}$CD4$^+$ CD45RB^{high} cells would easily be explained by the lack of a MyD88-dependent pathway in donor CD4$^+$ T cells, but not in other innate immune cells of the recipient mice.

At 6 wk after transfer, the colon from of mice transferred with MyD88$^{+/+}$ donor cells, but not that from mice transferred with MyD88$^{-/-}$ donor cells, was enlarged and had a greatly thickened wall (data not shown). In addition, the enlargement of the SP and MLN was also present in mice transferred with MyD88$^{+/+}$ donor cells as compared with mice transferred with MyD88$^{-/-}$ donor cells (data not shown). Histological examination revealed that mice transferred with MyD88$^{+/+}$ donor cells developed severe colitis showing prominent epithelial hyperplasia and erosion with a massive infiltration of mononuclear cells in LP of the colon (Fig. 2*D*). In contrast, mice transferred with MyD88$^{-/-}$ donor cells developed milder colitis as compared with mice transferred with MyD88$^{+/+}$ donor cells. This difference was statistically confirmed by histological scoring of multiple colon sections, which was mice transferred with MyD88$^{+/+}$ donor cells, 17.0 ± 1.0; and mice transferred with MyD88$^{-/-}$ donor cells, 6.2 ± 2.42 ($p < 0.01$) (Fig. 2*E*). Importantly, flow cytometry analysis revealed that the LP CD4$^+$ T cells isolated from recipients transferred with either MyD88$^{-/-}$ or MyD88$^{+/+}$ CD4$^+$CD45RB^{high} T cells were CD44^{high}CD62L$^-$IL-7Rα^{high} (Fig. 2*F*), indicating that the transferred CD4$^+$CD45RB^{high} T cells could differentiate into effector-memory T cells even in the absence of the MyD88-dependent pathway within colitic CD4$^+$ T cells.

A further quantitative evaluation of CD4$^+$ T cell infiltration was made by isolating LP, MLN, and SP CD3$^+$CD4$^+$ T cells. As shown in Fig. 2*G*, significantly lower numbers of CD4$^+$ T cells were recovered from LP, MLN, and SP of mice transferred with

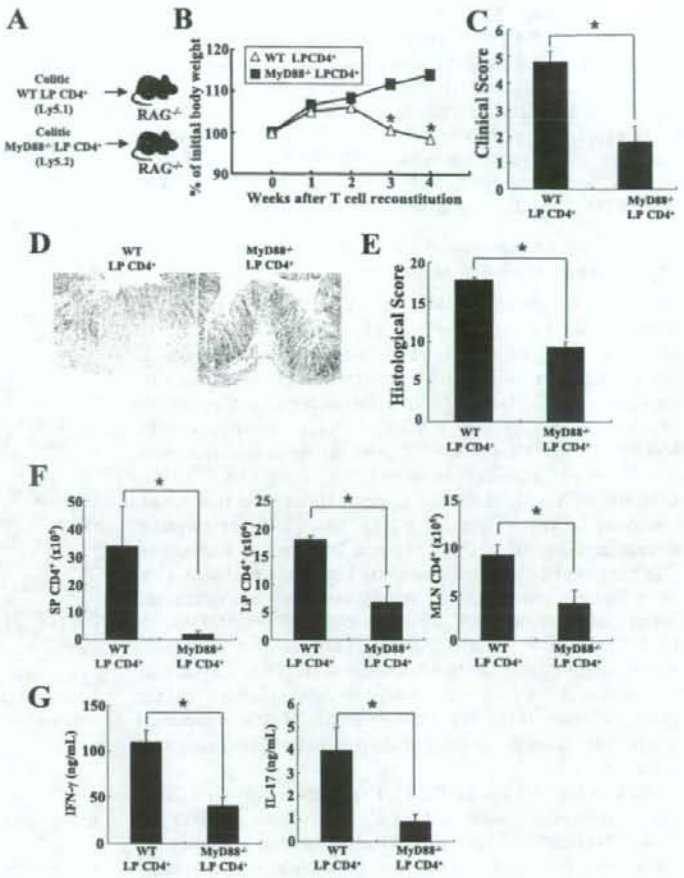

FIGURE 6. RAG-2$^{-/-}$ mice transferred with colitogenic MyD88$^{-/-}$ LP CD4$^+$ T cells develop milder colitis. *A*, RAG-2$^{-/-}$ mice were transferred with colitogenic MyD88$^{+/+}$ (WT) ($n = 6$) or MyD88$^{-/-}$ ($n = 6$) LP CD4$^+$ T cells (4×10^5 cells/mouse). *B*, Change in body weight is expressed as percent of the original weight. Data are represented as mean ± SEM of six mice in each group. *, $p < 0.05$. *C*, Clinical scores were determined at 4 wk after transfer as described in *Materials and Methods*. Data are indicated as mean ± SEM of six mice in each group. *, $p < 0.01$. *D*, Histological examination of the colon from mice transferred with colitic WT (*left*) or MyD88$^{-/-}$ (*right*) CD4$^+$ T cells at 4 wk after transfer. Original magnification, ×100. *E*, Histological scoring of mice transferred with colitic WT or MyD88$^{-/-}$CD4$^+$ T cells at 4 wk after transfer. Data are indicated as mean ± SEM of six mice in each group. *, $p < 0.05$. *F*, LP, MLN, and SP CD4$^+$ T cells were isolated from of mice transferred with colitic WT or MyD88$^{-/-}$CD4$^+$ T cells at 4 wk after transfer, and the number of CD4$^+$ cells was determined by flow cytometry. Data are indicated as mean ± SEM of six mice in each group. *, $p < 0.05$. *G*, Cytokine production by LP CD4$^+$ T cells. LP CD4$^+$ T cells were isolated at 4 wk after transfer and stimulated with anti-CD3 and -CD28 mAbs for 48 h. IFN-γ and IL-17 concentrations in culture supernatants were measured by ELISA. Data are indicated as mean ± SEM of six mice in each group. *, $p < 0.05$.

MyD88$^{-/-}$ donor cells as compared with mice transferred with MyD88$^{+/+}$ donor cells. To further address the survival of CD4$^+$ T cells, we next assessed whether regulation of Bcl-2 and Bcl-x_L expression requires the MyD88-dependent signaling pathway using a quantitative RT-PCR. As expected, the SP CD4$^+$ T cells from mice transferred with MyD88$^{-/-}$ donor cells expressed a significantly lower level of Bcl-2 and Bcl-x_L compared with those from mice transferred with MyD88$^{+/+}$ donor cells (Fig. 2*H*). We also examined the cytokine production by isolated LP CD4$^+$ T cells from recipient mice transferred with MyD88$^{+/+}$ or MyD88$^{-/-}$ donor cells along with LP CD4$^+$ T cells from healthy MyD88$^{+/+}$ or MyD88$^{-/-}$ mice. As shown in Fig. 2*I*, LP CD4$^+$ T cells from mice transferred with MyD88$^{-/-}$ donor cells produced significantly less IFN-γ and IL-17 as compared with those from mice transferred with MyD88$^{+/+}$ donor cells upon in vitro stimulation by anti-CD3/anti-CD28 mAbs. LP CD4$^+$ T cells from both healthy WT and MyD88$^{-/-}$ mice produced only a small amount of these cytokines, showing no significant difference under the same condition (Fig. 2*I*).

Vβ repertoire is almost constant regardless of WT or MyD88$^{-/-}$ donor cells

Although we found that mice transferred with MyD88$^{-/-}$ donor cells develop milder colitis compared with mice transferred with MyD88$^{+/+}$ donor cells, possibly due to the lack of a MyD88 pathway within CD4$^+$ T cells, it remained unclear whether expanded CD4$^+$ T cells in the recipient mice recognize the same antigenic epitopes of CD4$^+$ T cells. To clarify this issue, SP CD4$^+$ T cells from both groups of mice were analyzed for their TCR Vβ repertoire by flow cytometry. As shown in Fig. 3, the polyclonal dominant TCR Vβ repertoire with the dominancy of Vβ8.1/8.2 and Vβ8.3 was almost constant regardless of MyD88$^{+/+}$ or MyD88$^{-/-}$ donor cells. Only the frequency of Vβ5.1/5.2 in mice transferred with MyD88$^{-/-}$ donor cells was significantly increased as compared with that in mice transferred with WT donor cells, indicating that colitogenic CD4$^+$ T cells recognizing the same or similar Ag epitopes could develop independently from the TLR-MyD88 signaling pathway in CD4$^+$ T cells.

Expansive activity of WT donor cells predominates over that of MyD88$^{-/-}$ donor cells in in vivo competition assay

To further assess the requirement of TLR-MyD88 signaling for the expansion of CD4$^+$ donor cells, we performed in vivo competition experiments. The same number (2.5×10^5 cells/mouse) of CD4$^+$CD45RB^{high} donor cells from Ly5.1-background (Ly5.1$^+$) MyD88$^{+/+}$ and Ly5.2-background (Ly5.2$^+$) MyD88$^{-/-}$ mice were coinjected i.p. into the identical RAG-2$^{-/-}$ mice (Fig. 4*A*). As expected, recipient mice developed severe colitis at 6 wk after cotransfer (data not shown), and a significantly lower proportion of Ly5.2$^+$ MyD88$^{-/-}$ CD4$^+$ T cells was observed not only in the inflamed LP, but also in SP,

MLN, PB, and BM, as compared with the paired Ly5.1$^+$MyD88$^{+/+}$CD4$^+$ T cells (Fig. 4*B*). Furthermore, the ratio of IFN-γ-expressing cells within total MyD88$^{-/-}$ LP CD4$^+$ T cells was significantly lower compared with that in total MyD88$^{+/+}$ LP CD4$^+$ T cells (Fig. 4*C*). Consistent with the lower expression of IFN-γ in MyD88$^{-/-}$ LP CD4$^+$ T cells, expression of the activation marker CD69 on MyD88$^{-/-}$ LP or SP CD4$^+$ cells was significantly lower than on MyD88$^{+/+}$ LP or SP CD4$^+$ T cells, respectively (Fig. 4*D*).

RAG-2$^{-/-}$ mice transferred with MyD88$^{-/-}$ colitogenic LP CD4$^+$ donor cells develop milder colitis

To next assess the role of MyD88-dependent pathway in persistent colitis, we next examined colitogenic LP CD4$^+$ T cell-mediated colitis model (17), which lacks the impact of naive T cell priming, activation, and differentiation phase required in the former CD4$^+$CD45RB^{high} T cell-transferred colitis model. We first confirmed that RAG-2$^{-/-}$ mice transferred with MyD88$^{-/-}$CD4$^+$CD45RB^{high} T cells do develop colitis to a similar extent to mice transferred with MyD88$^{+/+}$CD4$^+$ CD45RB^{high} T cells at the late stage of 10 wk after transfer as confirmed by the weight curve (Fig. 5*A*), albeit the ongoing disease activity index (Fig. 5*B*) and histological assessment (Fig. 5, *C* and *D*) delayed onset and kinetics. Consistent with these findings, the recovered cell number was equivalent between mice transferred with MyD88$^{+/+}$ or MyD88$^{-/-}$ CD4$^+$CD45RB^{high} T cells (Fig. 5*E*). Furthermore, the expression of activation (CD69)/differentiation (IL-7Rα, CD44, and CD62L) on LP CD4$^+$ T cells showed no difference between two groups of mice (Fig. 5*F*), indicating that MyD88 deficiency solely contributes to the delayed kinetics of the development of colitis.

We thus isolated the LP CD4$^+$ T cells from colitic recipient mice transferred with either MyD88$^{+/+}$ or MyD88$^{-/-}$ CD4$^+$CD45RB^{high} T cells at 10 wk after transfer, to use for the subsequent memory T cell transfer. We transferred the isolated colitic LP CD4$^+$ T cells into new RAG-2$^{-/-}$ mice to focus on the persistence of colitogenic CD4$^+$ memory T cells (Fig. 6*A*). Similar with the results using CD4$^+$CD45RB^{high} T cell-mediated colitis model in Fig. 2, the recipient mice transferred with colitic MyD88$^{-/-}$ LP CD4$^+$ T cells showed milder wasting disease (Fig. 6*B*) with milder clinical signs of colitis at 4 wk after retransfer, as compared with mice transferred with colitic MyD88$^{+/+}$ LP CD4$^+$ T cells (Fig. 6*C*). Histological examination also revealed that mice transferred with MyD88$^{-/-}$ LP CD4$^+$ T cells developed milder colitis at 4 wk after retransfer as compared with mice transferred with MyD88$^{+/+}$ LP CD4$^+$ T cells (Fig. 6*D*). The difference was statistically confirmed by histological scoring of colon sections, which showed as follows: mice transferred with MyD88$^{+/+}$ LP CD4$^+$ T cells, 17.8 ± 0.86 and mice transferred with MyD88$^{-/-}$ LP CD4$^+$ T cells, 9.4 ± 1.86 ($p < 0.01$) (Fig. 6*E*). Furthermore, a significantly lower number of CD4$^+$ T cells was recovered from SP, LP, and MLN of mice transferred with MyD88$^{-/-}$ donor cells as compared with mice transferred with MyD88$^{+/+}$ donor cells (Fig. 6*F*). As shown in Fig. 6*G*, LP CD4$^+$ T cells from mice transferred with MyD88$^{-/-}$ LP donor cells produced significantly less IFN-γ and IL-17 as compared with those from mice transferred with MyD88$^{+/+}$ LP donor cells.

To further assess the expansive activity of colitic LP CD4$^+$ memory T cells, we again performed in vivo competition experiments. The same number (2.0×10^5 cells/mouse) of colitic Ly5.1$^+$MyD88$^{+/+}$ and Ly5.2$^+$MyD88$^{-/-}$ LP donor cells obtained from colitic mice transferred with Ly5.1$^+$MyD88$^{+/+}$ or Ly5.2$^+$MyD88$^{-/-}$ CD4$^+$CD45RB^{high} T cells at 10 wk after transfer was coinjected i.p. into identical RAG-2$^{-/-}$ mice (Fig. 7*A*). Six wk after cotransfer, a significantly lower proportion of Ly5.2$^+$ MyD88$^{-/-}$CD4$^+$ T cells was recovered from the inflamed LP, SP, and MLN, as compared with the paired Ly5.1$^+$MyD88$^{+/+}$CD4$^+$ T cells (Fig. 7*B*). Furthermore, the ratio of IFN-γ-expressing CD4$^+$ T cells within total MyD88$^{-/-}$ LP CD4$^+$ T cells was significantly decreased as compared with that within total MyD88$^{+/+}$ LP CD4$^+$ T cells (Fig. 7*C*).

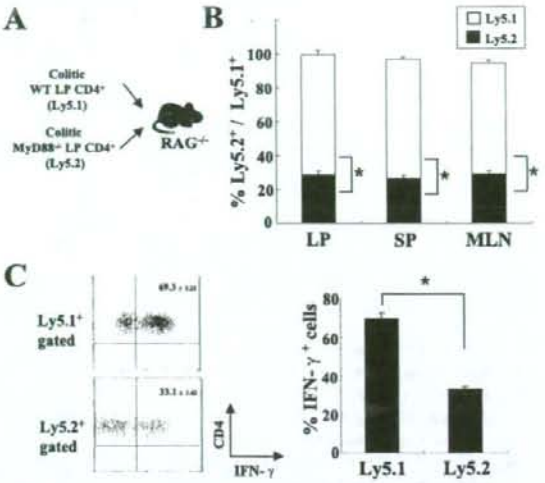

FIGURE 7. Expansion activity of colitic MyD88$^{+/+}$ LP donor cells predominates over that of MyD88$^{-/-}$ donor cells in an in vivo competition assay. *A*, The same number (2.0×10^5 cells/mouse) of colitic LP MyD88$^{+/+}$ (WT) (Ly5.1$^+$) and MyD88$^{-/-}$ (Ly5.2$^+$) CD4$^+$ T cells mice was injected i.p. into RAG-2$^{-/-}$ mice ($n = 6$). *B*, Six weeks after transfer, LP, SP, and MLN CD4$^+$ T cells were isolated from mice, and the ratio of Ly5.1$^+$ and Ly5.2$^+$ CD4$^+$ cells was determined by flow cytometry. *, $p < 0.01$. *C*, The frequencies of IFN-γ-producing cells per the total Ly5.1$^+$ or Ly5.2$^+$ cells were analyzed in the indicated subpopulations by flow cytometry. Data are represented as mean ± SEM of three independent experiments. *, $p < 0.01$.

MyD88 signaling contributes to the lymphopenia-driven rapid proliferation of colitogenic CD4$^+$ T cells

To finally examine the effect of MyD88 signaling on the lymphopenia-driven rapid proliferation (18) of the colitogenic CD4$^+$ memory T cells, we used the in vivo CFSE dilution method to examine cells undergoing proliferation after a short period from transfer. First, the LP CD4$^+$ T cells obtained from colitic RAG-2$^{-/-}$ mice transferred with either MyD88$^{+/+}$ or MyD88$^{-/-}$ CD4$^+$CD45RB^{high} T cells at 10 wk after transfer were labeled with CFSE and adoptively cotransferred into new RAG-2$^{-/-}$ mice. Cell divisions were determined 10 days after cotransfer by assessing the CFSE dilution (Fig. 8*A*). As depicted in Fig. 8*B*, the markedly delayed division pattern of CD4$^+$ T cells from mice transferred with MyD88$^{-/-}$ donor cells was observed as compared with that in mice transferred with MyD88$^{+/+}$ donor cells. This difference was statistically confirmed by comparing the CFSE$^+$ cells between Ly5.1$^+$ and Ly5.2$^+$ cells (Fig. 8*C*), indicating that the MyD88-dependent signaling pathway in T cells promotes the rapid proliferation of colitogenic CD4$^+$ memory T cells in a lymphopenic condition.

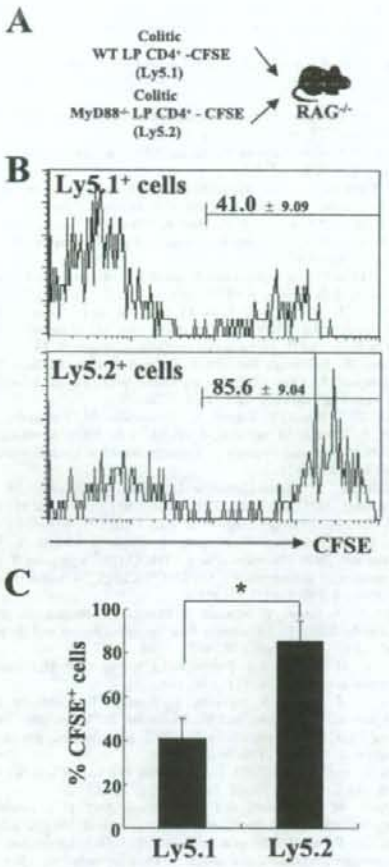

FIGURE 8. MyD88 pathway contributes to the lymphopenia-driven rapid proliferation of colitogenic $CD4^+$ T cells. *A*, The same number (2.0×10^6 cells/mouse) of CFSE-labeled colitic LP $MyD88^{+/+}$ (WT) ($Ly5.1^+$) and $MyD88^{-/-}$ ($Ly5.2^+$) $CD4^+$ T cells were coinjected i.p. into new RAG-$2^{-/-}$ mice ($n = 6$). *B*, The donor cells in the host spleen were analyzed 10 days after transfer by staining CD4, Ly5.1, and Ly5.2. Histograms show CFSE profiles of the two donor cell types in the host spleen. Data are representative of five independent experiments. *C*, Percentages of positive CFSE staining per total $Ly5.1^+$ or $Ly5.2^+$ cells were analyzed in the indicated subpopulations by flow cytometry. Data are represented as mean ± SEM of three independent experiments. *, $p < 0.05$.

Discussion

In the present study, we demonstrated that the MyD88-dependent signaling pathway in T cells directly modulates the proliferation and survival of TLRs/MyD88-expressing colitogenic $CD4^+$ T cells during the development and persistence of colitis. So far, it has been believed that T cell activation and expansion is induced and maintained by TCR signaling through the interaction with Ag-loading DCs that are primarily activated by PAMP/TLR-induced maturation (21). However, this study provides a new pathway by which the MyD88-dependent signaling pathway within $CD4^+$ T cells may directly play a pivotal role in the acquired immune components of chronic colitis by enhancing PAMP-specific immune responses collaborating with Ag-specific TCR signaling and homeostatic cytokines, such as IL-7 and IL-15 (18, 22–24).

How do commensal bacteria-derived PAMPs contribute to the maintenance of colitogenic $CD4^+$ T cells during the perpetuation of colitis? In other words, from where do colitogenic $CD4^+$ T cells receive proliferative and/or survival signals to sustain chronic colitis? First, it is well-known that commensal bacteria are essentially required for the development and the persistence of colitis, because 1) almost all models of T cell-mediated colitis do not develop colitis under the germfree condition (4–6), and 2) several groups elegantly demonstrated the requirement of specific Ags for the development and persistence of colitis by showing that colitis is induced and sustained by administration of OVA peptide-expressing *Escherichia coli* into OVA-specific TCR-transgenic mice in an Ag-specific manner (25, 26). These results indicated that TCR signaling through Ags, especially Ags derived from commensals, are needed for the development and persistence of colitis. Second, in addition to Ags derived from commensal bacteria, we here showed that the MyD88-dependent signaling pathway directly bolsters up the proliferation and survival of colitogenic $CD4^+$ T cells. However, it is of note that RAG-$2^{-/-}$ mice transferred with $MyD88^{-/-}$ $CD4^+CD45RB^{high}$ T cells did develop colitis with $CD4^+$ T cell infiltration in the inflamed mucosa albeit the onset was delayed as compared with the control, indicating that the direct MyD88-dependent signaling pathway in colitogenic $CD4^+$ T cells may act as a costimulator to tune the essential TCR signaling for the maintenance of these cells. However, at the molecular level, it still remains unknown how the identical $CD4^+$ T cells coordinate TCR and TLR signaling initiated from the commensal bacteria for activation, proliferation, and survival. Further studies will be required to address this important issue.

So far, most studies regarding TLRs have focused on cells of the innate immune system, such as DCs, macrophages, and epithelial cells, and now it is recognized that members of TLRs play an essential role in the innate immune recognition allowing the detection of commensal bacteria, followed by the second activation of T cells (9–11). However, recent works showed that conventional TCR $\alpha\beta^+CD4^+$ T cells also express TLRs (12), suggesting that PAMPs may directly modulate the function of $CD4^+$ T cells. Importantly, Gelman et al. (27) recently reported that TLR signaling in primary $CD4^+$ T cells directly enhances proliferation through MyD88 and PI3K-dependent pathway, in response to a T cell-dependent Ag. Thus, the present study may add the identification of the role of TLR signaling in the activation/function of the pathogenic memory $CD4^+$ T cells. Although we showed that the MyD88-dependent signaling pathway positively reinforces the proliferation and survival of colitogenic $CD4^+$ T cells in colitic mice, it has been previously reported that TLR-4 is predominantly expressed on regulatory $CD4^+CD25^+$ T cells rather than $CD4^+CD45RB^{high}$ naive cells, and TLR-4-specific signaling by LPS increases the regulatory $CD4^+CD25^+$ T cell activity, resulting in suppression of inflammatory responses in vivo (16). We slightly, but substantially, detected TLR-4 mRNA as well as other TLRs in colitic LP $CD4^+$ T cells, thus it is interesting to know how the stimulatory and inhibitory TLR-signaling pathway in T cells orchestrates the complicated immune responses in chronic colitis.

Such characteristics of TLR/MyD88-expressing colitogenic $CD4^+$ T cells raise another important question of whether the colitogenic $CD4^+CD44^{high}CD62L^-IL\text{-}7R\alpha^{high}$ T cells (Fig. 2) can be defined as effector-memory T cells rather than just effector T cells under the persistent presence of commensal Ags and/or self Ags, because it is accepted that memory T cells are generated after Ag clearance for the first time, but not under persistent presence of Ags, shown in models of chronic viral infections to $CD8^+$ T cells, using lymphocytic choriomeningitis virus or influenza A virus infections (28). Because the candidate Ags for colitogenic $CD4^+$ T cells are thought to be derived

from the intestinal bacterial Ags that are never eliminated from the body, it is doubtful whether colitogenic $CD4^+$ memory T cells can be generated under such a situation. However, as recent studies have suggested that persistent presence of Ags is rather required for the long-term maintenance of $CD4^+$ memory T cells, it is possible that the nature of $CD4^+$ memory T cells is quite different from that of $CD8^+$ memory T cells (29, 30). Thus, the present results may support another idea that the persistent presence of both commensal bacteria-derived PAMPs and specific Ags is required for the maintenance of long-term colitogenic $CD4^+$ memory T cells, and the subsequent progressive, disabling disease course.

It is also possible that nonpathogenic commensals stimulate TLR signaling of colitogenic $CD4^+$ memory T cells to sustain the disease without providing specific Ags for such cells. In other words, it should be verified whether specific Ags or PAMPs from the commensal bacteria are essential for the priming or memory phase. Consistently, the current study also provides an explanation of why a common recurrence of IBD is observed during complication of microbial infection, such as acute *Salmonella enterocolitis*, which may possibly supply large amounts of "bystander" PAMPs (31).

Finally, an important point should also be discussed: whether the present experimental design solely assesses the role of direct TLR signaling in various stages of $CD4^+$ T cells during the development of chronic colitis, because MyD88 is also involved in signaling downstream of endogenous cytokines, IL-1 and IL-18, in addition to TLR signaling (13, 14). Further studies will be required to address this issue by assessing which TLR is the most important for the stimulation of colitogenic $CD4^+$ T cells, followed by in vivo experiment using the corresponding TLR^{null} mice.

In summary, we here demonstrate that the MyD88-dependent pathway that mediates downstream signals of TLRs is crucially involved in the proliferative and survival responses of colitogenic $CD4^+$ T cells, which is required for the perpetuation of chronic colitis. Thus, in addition to the specific commensal Ags, homeostatic cytokines, and costimulatory molecules, therapeutic approaches targeting PAMPs may be feasible in the treatment of IBD.

Disclosures

The authors have no financial conflict of interest.

References

1. Podolsky, D. K. 2002. Inflammatory bowel disease. *N. Engl. J. Med.* 347: 417–429.
2. Baumgart, D. C., and S. R. Carding. 2007. Inflammatory bowel disease: cause and immunobiology. *Lancet* 369: 1627–1640.
3. Strober, W., I. J. Fuss, and R. S. Blumberg. 2002. The immunology of mucosal models of inflammation. *Annu. Rev. Immunol.* 20: 495–549.
4. Seksik, P., H. Sokol, P. Lepage, N. Vasquez, C. Manichanh, I. Mangin, P. Pochart, J. Dore, and P. Marteau. 2006. Review article: the role of bacteria in onset and perpetuation of inflammatory bowel disease. *Aliment. Pharmacol. Ther.* 24(Suppl. 3): 11–18.
5. Sartor, R. B. 2006. Mechanisms of disease: pathogenesis of Crohn's disease and ulcerative colitis. *Nat. Clin. Pract. Gastroenterol. Hepatol.* 3: 390–407.
6. Izcue, A., J. L. Coombes, and F. Powrie. 2006. Regulatory T cells suppress systemic and mucosal immune activation to control intestinal inflammation. *Immunol. Rev.* 212: 256–271.
7. Bamias, G., M. R. Nyce, S. A. De La Rue, and F. Cominelli. 2005. New concepts in the pathophysiology of inflammatory bowel disease. *Ann. Intern. Med.* 143: 895–904.
8. Hibi, T., and H. Ogata. 2006. Novel pathophysiological concepts of inflammatory bowel disease. *J. Gastroenterol.* 41: 10–16.
9. Akira, S., S. Uematsu, and O. Takeuchi. 2006. Pathogen recognition and innate immunity. *Cell* 124: 783–801.
10. Rakoff-Nahoum, S., and R. Medzhitov. 2006. Role of the innate immune system and host-commensal mutualism. *Curr. Top. Microbiol. Immunol.* 308: 1–18.
11. Schnare, M., G. M. Barton, A. C. Holt, K. Takeda, S. Akira, and R. Medzhitov. 2001. Toll-like receptors control activation of adaptive immune responses. *Nat. Immunol.* 2: 947–950.
12. Kabelitz, D. 2007. Expression and function of Toll-like receptors in T lymphocytes. *Curr. Opin. Immunol.* 19: 39–45.
13. Adachi, O., T. Kawai, K. Takeda, M. Matsumoto, H. Tsutsui, M. Sakagami, K. Nakanishi, and S. Akira. 1998. Targeted disruption of the *MyD88* gene results in loss of IL-1- and IL-18-mediated function. *Immunity* 9: 143–150.
14. Medzhitov, R., P. Preston-Hurlburt, E. Kopp, A. Stadlen, C. Chen, S. Ghosh, and C. A. Janeway, Jr. 1998. MyD88 is an adaptor protein in the hToll/IL-1 receptor family signaling pathways. *Mol. Cell* 2: 50–53.
15. Totsuka, T., T. Kanai, R. Iiyama, K. Uraushihara, M. Yamazaki, R. Okamoto, T. Hibi, K. Tezuka, M. Azuma, H. Akiba, et al. 2003. Ameliorating effect of anti-ICOS monoclonal antibody in a murine model of chronic colitis. *Gastroenterology* 124: 410–421.
16. Caramalho, I., T. Lopes-Carvalho, D. Ostler, S. Zelenay, M. Haury, and J. Demengeot. 2003. Regulatory T cells selectively express toll-like receptors and are activated by lipopolysaccharide. *J. Exp. Med.* 197: 403–411.
17. Kanai, T., K. Tanimoto, Y. Nemoto, R. Fujii, S. Makita, T. Totsuka, and M. Watanabe. 2006. Naturally arising $CD4^+CD25^+$ regulatory T cells suppress the expansion of colitogenic $CD4^+CD44^{high}CD62L^-$ effector memory T cells. *Am. J. Physiol.* 290: G1051–G1058.
18. Totsuka, T., T. Kanai, Y. Nemoto, S. Makita, R. Okamoto, K. Tsuchiya, and M. Watanabe. 2007. IL-7 is essential for the development and the persistence of chronic colitis. *J. Immunol.* 178: 4737–4748.
19. Surh, C. D., O. Boyman, J. F. Purton, and J. Sprent. 2006. Homeostasis of memory T cells. *Immunol. Rev.* 211: 154–163.
20. Makita, S., T. Kanai, Y. Nemoto, T. Totsuka, R. Okamoto, K. Tsuchiya, M. Yamamoto, H. Kiyono, and M. Watanabe. 2007. Intestinal lamina propria retaining $CD4^+CD25^+$ regulatory T cells is a suppressive site of intestinal inflammation. *J. Immunol.* 178: 4937–4946.
21. Kaisho, T., and S. Akira. 2001. Dendritic-cell function in Toll-like receptor- and MyD88-knockout mice. *Trends Immunol.* 22: 78–83.
22. Bradley, L. M., L. Haynes, and S. L. Swain. 2005. IL-7: maintaining T-cell memory and achieving homeostasis. *Trends Immunol.* 26: 172–176.
23. Seddon, B., P. Tomlinson, and R. Zamoyska. 2003. Interleukin 7 and T cell receptor signals regulate homeostasis of CD4 memory cells. *Nat. Immunol.* 4: 680–686.
24. Picker, L. J., E. F. Reed-Inderbitzin, S. I. Hagen, J. B. Edgar, S. G. Hansen, A. Legasse, S. Planer, M. Piatak, Jr., J. D. Lifson, V. C. Maino, et al. 2006. IL-15 induces CD4 effector memory T cell production and tissue emigration in nonhuman primates. *J. Clin. Invest.* 116: 1514–1524.
25. Iqbal, N., J. R. Oliver, F. H. Wagner, A. S. Lazenby, C. O. Elson, and C. T. Weaver. 2002. T helper 1 and T helper 2 cells are pathogenic in an antigen-specific model of colitis. *J. Exp. Med.* 195: 71–84.
26. Yoshida, M., T. Watanabe, T. Usui, Y. Matsunaga, Y. Shirai, M. Yamori, T. Itoh, S. Habu, T. Chiba, T. Kita, and Y. Wakatsuki. 2001. T cells monospecific to ovalbumin produced by *Escherichia coli* can induce colitis upon transfer to BALB/c and SCID mice. *Int. Immunol.* 13: 1561–1570.
27. Gelman, A. E., D. F. LaRosa, J. Zhang, P. T. Walsh, Y. Choi, J. O. Sunyer, and L. A. Turka. 2006. The adaptor molecule MyD88 activates PI-3 kinase signaling in $CD4^+$ T cells and enables CpG oligodeoxynucleotide-mediated costimulation. *Immunity* 25: 783–793.
28. Klenerman, P., and A. Hill. 2005. T cells and viral persistence: lessons from diverse infections. *Nat. Immunol.* 6: 873–879.
29. Robertson, J. M., M. MacLeod, V. S. Marsden, J. W. Kappler, and P. Marrack. 2006. Not all $CD4^+$ memory T cells are long lived. *Immunol. Rev.* 211: 49–57.
30. Zaph, C., J. Uzonna, S. M. Beverley, and P. Scott. 2004. Central memory T cells mediate long-term immunity to Leishmania major in the absence of persistent parasites. *Nat. Med.* 10: 1104–1110.
31. Stallmach, A., and O. Carstens. 2002. Role of infections in the manifestation or reactivation of inflammatory bowel diseases. *Inflamm. Bowel. Dis.* 8: 213–218.

0022-3565/09/3281-152–164$20.00
THE JOURNAL OF PHARMACOLOGY AND EXPERIMENTAL THERAPEUTICS

JPET 328:152–164, 2009

Vol. 328, No. 1
144451/3420793
Printed in U.S.A.

Therapeutic Effect of Lecithinized Superoxide Dismutase against Colitis

Tomoaki Ishihara, Ken-Ichiro Tanaka, Yuichi Tasaka, Takushi Namba, Jun Suzuki, Tsutomu Ishihara, Susumu Okamoto, Toshifumi Hibi, Mitsuko Takenaga, Rie Igarashi, Keizo Sato, Yutaka Mizushima, and Tohru Mizushima

Graduate School of Medical and Pharmaceutical Sciences, Kumamoto University, Kumamoto, Japan (T.I., K.-I.T., Y.T., T.N., J.S., T.I., K.S., T.M.); DDS Institute, The Jikei University School of Medicine, Tokyo, Japan (T.I., Y.M.); Department of Internal Medicine, Keio University School of Medicine, Tokyo, Japan (S.O., T.H.); and Division of Drug Delivery System, Institute of Medical Science, St. Marianna University, Kawasaki, Japan (M.T., R.I.)

Received August 5, 2008; accepted October 15, 2008

ABSTRACT

Ulcerative colitis (UC) involves intestinal mucosal damage induced by reactive oxygen species (ROS), in particular, superoxide anion. Superoxide dismutase (SOD) catalyzes dismutation of superoxide anion to hydrogen peroxide, which is subsequently detoxified by catalase. Lecithinized SOD (PC-SOD) is a new modified form of SOD that has overcome previous clinical limitations of SOD. In this study, we examined the action of PC-SOD using an animal model of UC, dextran sulfate sodium (DSS)-induced colitis. DSS-induced colitis was ameliorated by daily intravenous administration of PC-SOD. Unmodified SOD produced a similar effect but only at more than 30 times the concentration of PC-SOD. In vivo electron spin resonance analysis confirmed that the increase in the colonic level of ROS associated with development of colitis was suppressed by PC-SOD administration. The dose-response profile of PC-SOD was bell-shaped, but simultaneous administration of catalase restored the ameliorative effect at high doses of PC-SOD. Accumulation of hydrogen peroxide was observed with the administration of high doses of PC-SOD, an effect that was suppressed by the simultaneous administration of catalase. We also found that either a weekly intravenous administration or daily oral administration of PC-SOD conferred protection. These results suggest that PC-SOD achieves its ameliorative effect against colitis through decreasing the colonic level of ROS and that its ineffectiveness at higher doses is because of the accumulation of hydrogen peroxide. Furthermore, we consider that intermittent or oral administration of PC-SOD can be applied clinically to improve the quality of life of UC patients.

Inflammatory bowel disease (IBD), Crohn's disease, and ulcerative colitis (UC) have become substantial health problems (Cuzzocrea, 2003). Recent studies suggest that IBD is chronic inflammatory disorder occurs in the intestine because of "a vicious cycle"; infiltration of leukocytes into intestinal tissues causes mucosal damage induced by reactive oxygen species (ROS) that are released from the activated leukocytes, and this damage further stimulates the infiltration of leukocytes through induction of proinflammatory cytokines, in particular, tumor necrosis factor (TNF)-α (Podolsky, 2002). Among the various ROS, superoxide anion is particularly important because it has a potent ability to damage cells and leads to the formation of other ROS, such as hydroxy radicals (Kruidenier and Verspaget, 2002). A positive correlation between the severity of IBD and the intestinal level of ROS has been reported (Simmonds et al., 1992). Thus, antioxidant molecules (radical scavengers) have attracted considerable attention as therapeutic candidates for the treatment of IBD.

Superoxide dismutase (SOD) is one such antioxidant protein. SOD catalyzes the dismutation of superoxide anion to

This work was supported by Grant-in-Aid for Scientific Research #H20-004 from the Ministry of Health, Labor, and Welfare of Japan, Grant H19-331-1 from Japan Science and Technology Agency, and Grant-in-Aid for Scientific Research #181013043 from the Ministry of Education, Culture, Sports, Science and Technology of Japan.

Article, publication date, and citation information can be found at http://jpet.aspetjournals.org.

doi:10.1124/jpet.108.144451.

ABBREVIATIONS: IBD, inflammatory bowel disease; UC, ulcerative colitis; ROS, reactive oxygen species; TNF, tumor necrosis factor; SOD, superoxide dismutase; PC-SOD, lecithinized superoxide dismutase; DSS, dextran sulfate sodium; DAI, disease activity index; U-SOD, unmodified superoxide dismutase; QOL, quality of life; ESR, electron spin resonance; PMA, phorbol 12-myristate 13-acetate; LPS, lipopolysaccharide; DMPO, 5,5-dimethyl-1-pyrroline-*N*-oxide; RT, reverse transcriptase; PCR, polymerase chain reaction; POBN, α-(4-pyridyl-1-oxide)-*N*-*tert*-butylnitrone; DTPA, diethylenetriamine-*N*,*N*,*N*′,*N*″,*N*″-pentaactic acid; DAPI, 4,6-diamidino-2-phenylindole; NF, nuclear factor; MPO, myeloperoxidase; GAPDH, glyceraldehyde-3-phosphate dehydrogenase; IL, interleukin; CL, chemiluminescence; ELISA, enzyme-linked immunosorbent assay.

hydrogen peroxide, which is subsequently detoxified to oxygen and water by catalase or glutathione peroxidase (Kruidenier and Verspaget, 2002). Among three isoforms of human SOD, Cu/Zn-SOD mainly contributes to the SOD activity in IBD patients (Kruidenier et al., 2003a). Decreased expression of SOD, especially Cu/Zn-SOD, has been observed in IBD patients (Kruidenier et al., 2003a,b). Furthermore, administration of Cu/Zn-SOD suppresses the development of IBD-related colitis in the experimental animal models (Keshavarzian et al., 1990; Segui et al., 2004). These findings raised the prospect that SOD could be of therapeutic benefit in the treatment of IBD. However, subsequent clinical trials of Cu/Zn-SOD have proven unsuccessful, mostly because of its low affinity to the cell membrane, where superoxide anion is produced, and its low stability in plasma, with a half-life of only a few minutes (Greenwald, 1990; Tsao et al., 1991; Igarashi et al., 1992, 1994). Therefore, various drug delivery systems have been applied to SOD to overcome these limitations (Keshavarzian et al., 1990; Igarashi et al., 1992, 1994; Yasui and Baba, 2006).

Among these applications, lecithinized SOD (PC-SOD) is potentially beneficial for clinical treatment of IBD, especially UC. PC-SOD is lecithinized human Cu/Zn-SOD, in which four phosphatidylcholine-derivative molecules are covalently bound to each SOD dimer (Igarashi et al., 1992). In vitro experiments using cultured cells have shown that this modification drastically improves the cell membrane affinity of SOD without decreasing its SOD activity (Igarashi et al., 1992, 1994), whereas in vivo experiments using rats have demonstrated that it also greatly improves plasma stability (Igarashi et al., 1992). In phase I clinical studies, intravenously administered PC-SOD (40–160 mg) had a terminal half-life of more than 24 h, with good safety and tolerability (Broeyer et al., 2008; Suzuki et al., 2008a). Furthermore, intravenously administered PC-SOD ameliorated dextran sulfate sodium (DSS)-induced colitis in rats, an IBD-related colitis animal model (Hori et al., 1997), suggesting that PC-SOD is effective for the treatment of IBD patients. In fact, recent published results of phase II clinical study have shown that intravenously administered PC-SOD (40 or 80 mg) significantly improved the disease activity index (DAI) scores of UC patients (Suzuki et al., 2008b). However, the comparison of PC-SOD with unmodified SOD (U-SOD) based on pharmacological activity against colitis has not been undertaken, and a decrease in the ROS level with PC-SOD administration has not been demonstrated in vivo. In addition to U-SOD, a bell-shaped dose-response profile of PC-SOD has been reported for various pharmacological activities, including anticolitis activity (Mao et al., 1993; Hori et al., 1997; Tamagawa et al., 2000; Tsubokawa et al., 2007). However, its underlying mechanism has remained unknown. Furthermore, when considering the quality of life (QOL) of patients, the present clinical protocol of PC-SOD administration (intravenous infusion once daily for 4 weeks) is expected to be improved. In this study, we compared PC-SOD and U-SOD for their pharmacological activity against DSS-induced colitis and found that PC-SOD has more than 30 times higher activity. In vivo electron spin resonance (ESR) analysis showed that administration of PC-SOD suppressed the increase in the ROS level induced by DSS treatment. We also provide evidence that the ineffectiveness of higher doses of PC-SOD is because of accumulation of hydrogen peroxide at the intestine. Furthermore, based on results obtained here, we propose that intermittent administration or oral administration of PC-SOD is a clinically viable option to improve the QOL of UC patients.

Materials and Methods

Chemicals and Animals. Paraformaldehyde, *O*-dianisidine, phorbol 12-myristate 13-acetate (PMA), fetal bovine serum, and catalase from bovine liver (1340 U/mg) were obtained from Sigma-Aldrich (St. Louis, MO). RPMI 1640 was from Nissui (Tokyo, Japan). Enzymatic digest of animal tissue (Proteose peptone) was from BD Biosciences (San Jose, CA). LPS was from List Biological Laboratories Inc. (Campbell, CA). Alexa Fluor 488 goat anti-rabbit immunoglobulin G was purchased from Invitrogen (Carlsbad, CA). Mounting medium for immunohistochemical analysis (Vectashield) was from Vector Laboratories (Burlingame, CA). 5,5-Dimethyl-1-pyrroline-*N*-oxide (DMPO) was purchased from Labotec (Midrand, South Africa), lymphocyte isolation sterile solution (Ficoll-Paque PluS) from GE Healthcare (Chalfont St. Giles, UK), DSS (mol. wt., 5000; 15–20% sulfur content) and luminol from Wako Pure Chemicals (Tokyo, Japan), and Mayer's hematoxylin, 1% eosin alcohol solution, and mounting medium for histological examination (Malinol) from MUTO Pure Chemicals (Tokyo, Japan). The RNeasy kit was obtained from QIAGEN (Valencia, CA), the PrimeScript 1st strand cDNA Synthesis Kit was purchased from Takara (Kyoto, Japan), and mix for real-time RT-PCR (iQ SYBR Green Supermix) was from Bio-Rad Laboratories (Hercules, CA). α-(4-Pyridyl-1-oxide)-*N*-*tert*-butylnitrone (POBN) was from Alexis Laboratories (San Diego, CA). U-SOD (5190 U/mg) and PC-SOD (3000 U/mg) were from our laboratory stock (Igarashi et al., 1992). SODs were dissolved in 5% xylitol and administered intravenously (tail vein) or orally. Diethylenetriamine-*N*,*N*,*N*′,*N*″,*N*″-pentaactic acid (DTPA) and 4,6-diamidino-2-phenylindole (DAPI) were from DOJINDO Laboratories (Kumamoto, Japan). An antibody against phospho-nuclear factor (NF) κB p65 (Ser536) was from Cell Signaling Technology Inc. (Danvers, MA). Wild-type mice (8 weeks old, ICR, male) were used throughout. The experiments and procedures described here were carried out in accordance with the *Guide for the Care and Use of Laboratory Animals* as adopted and promulgated by the National Institutes of Health (Institute of Laboratory Animal Resources, 1996) and were approved by the Animal Care Committee of Kumamoto University.

Development of DSS-Induced Colitis and Measurement of Colon Length and DAI. DSS-induced colitis was induced in mice by the addition of 4% DSS (w/v, final concentration) to their drinking water as described previously (Tanaka et al., 2007). The first administration of PC-SOD was done just before the start of DSS administration. The animals were allowed free access to the DSS-containing water for 7 days. For measurement of myeloperoxidase (MPO) activity, expression of mRNAs, and the ROS level, we used rectum and distal colon tissue. After 7 days, animals were placed under deep ether anesthesia and sacrificed, the colons were dissected, and their length was measured from the ileocecal junction to the anal verge.

The DAI was determined macroscopically by an observer unaware of the treatment the mice had received, according to previously reported criteria (Tanaka et al., 2007). In brief, the DAI was calculated as the sum of the diarrheal stool score (0, normal stool; 1, mildly soft stool; 2, very soft stool; 3, watery stool) and the bloody stool score (0, normally colored stool; 1, brown stool; 2, reddish stool; 3, bloody stool).

MPO Activity. MPO activity in the colonic tissues was measured as previously described (Tanaka et al., 2007). After DSS treatment, colons were dissected, rinsed with cold saline, and cut into small pieces. Samples were homogenized, and protein concentrations of the samples were determined using the Bradford method. MPO activity was determined in 10 mM phosphate buffer with 0.5 mM *O*-dianisidine, 0.00005% (w/v) hydrogen peroxide, and 20 μg of protein. MPO activity was obtained from the slope of the reaction curve, and

specific activity was expressed as the number of hydrogen peroxide molecules converted per minute per milligram of protein.

Real-Time RT-PCR Analysis. Real-time RT-PCR was performed as previously described (Mima et al., 2005), with some modifications. Total RNA was extracted from intestinal tissues or mouse peritoneal macrophages using an RNeasy kit according to the manufacturer's protocol. Samples (2.5 μg of RNA) were reverse-transcribed using a first-strand cDNA synthesis kit. Synthesized cDNA was used in real-time RT-PCR (Chromo 4 instrument; Bio-Rad Laboratories) experiments using mix for real time RT-PCR and analyzed with Opticon Monitor Software. Specificity was confirmed by electrophoretic analysis of the reaction products and by inclusion of template- or reverse transcriptase-free controls. To normalize the amount of total RNA present in each reaction, glyceraldehyde-3-phosphate dehydrogenase (GAPDH) cDNA was used as an internal standard.

Primers were designed using the Primer3 Web site (http://frodo.wi.mit.edu/cgi-bin/primer3/primer3_www.cgi). The primers used were as follows: *Tnf*-α, 5′-cgtcagccgatttgctatct-3′ (forward) and 5′-cggactccgcaaagtctaag-3′ (reverse); *Gapdh*, 5′-aactttggcattgtggaagg-3′ (forward) and 5′-acacattgggggtaggaaca-3′ (reverse); *Il-1*β, 5′-gatcccaagcaatacccaaa-3′ (forward) and 5′-ggggaactctgcagactcaa-3′ (reverse); *Il-6*, 5′-ctggagtcacagaaggagtgg-3′ (forward) and 5′-ggtttgccgagtagatctcaa-3′ (reverse); and *Il-23p19*, 5′-gccccgtatccagtgtgaag-3′ (forward) and 5′-cggatcctttgcaagcagaa-3′ (reverse).

Histological and Immunohistochemical Analysis. Colonic tissue samples were fixed in 4% buffered paraformaldehyde, then embedded in paraffin before being cut into 4-μm sections. For histological examination, sections were stained first with Mayer's hematoxylin and then with 1% eosin alcohol solution. Samples were mounted with mounting medium and inspected with the aid of an Olympus BX51 microscope (Olympus, Tokyo, Japan).

For immunohistochemical analysis, sections were blocked with 3% bovine serum albumin for 30 min, incubated for 12 h with antibody against phospho-NF-κB (1:100 dilution) in the presence of 2.5% bovine serum albumin, and finally incubated for 1 h with Alexa Fluor 488 goat anti-mouse immunoglobulin G in the presence of DAPI (5 μg/ml). Samples were mounted with mounting medium and inspected using fluorescence microscopy (Olympus BX51).

Measurement of ROS in Neutrophils in Vitro. Human neutrophils were prepared as described previously (Karakawa et al., 2008). In brief, polymorphonuclear leukocytes and mononuclear cells were separated using a gradient of lymphocyte isolation sterile solution. Red blood cells remaining in the polymorphonuclear leukocyte fractions were lysed with 0.2% NaCl.

The chemiluminescence (CL) response induced by the superoxide anion released from neutrophils was measured as described (Muranaka et al., 1997). Prepared neutrophils were mixed with 25 ng/ml PMA in RPMI 1640 medium containing 10 μM luminol and 500 μM DTPA. The CL response was continuously recorded for 10 min at room temperature using a luminometer (Advantec Co., Tokyo, Japan).

The level of superoxide anion was also assayed by ESR spin trapping with DMPO as previously described (Karakawa et al., 2008). Prepared neutrophils were incubated with 10 ng/ml PMA in RPMI 1640 medium containing 500 μM DTPA and 25 mM DMPO for 5 min at room temperature. ESR spectra were recorded at room temperature on a JES-TE200 ESR spectrometer (JEOL, Tokyo, Japan) under the following conditions: modulation frequency, 100 kHz; microwave frequency, 9.43 GHz; microwave power, 40 mW; scanning field, 335.2 ± 5 mT; sweep time, 2 min; field modulation width, 0.25 mT; receiver gain, 100; and time count, 0.3 s. After recording the ESR spectra, the signal intensities of the DMPO-OOH adducts were normalized against that of a manganese oxide marker.

Determination of ROS Level and the Amount of Hydrogen Peroxide in Vivo. In vivo ESR analysis was performed as described previously (Sato et al., 1992, 2002), with some modifications. After DSS administration for 7 days, animals were placed under deep anesthesia with chloral hydrate (250 mg/kg) and injected with POBN intraperitoneally (4 mmol/kg). After 1 h, mice were sacrificed, the colons were dissected, and the lipid phase from the samples was extracted as described elsewhere (Sato et al., 1992, 2002). After evaporating the sample, ESR spectra were immediately recorded at room temperature in a JES-TE200 spectrometer under the following conditions: modulation frequency, 100 kHz; microwave frequency, 9.43 GHz; microwave power, 40 mW; scanning field, 335.2 ± 5 mT; sweep time, 2 min; field modulation width, 0.25 mT; receiver gain, 630; and time count, 0.3 s. Every buffer and solutions of the reaction mixture used for ESR measurement were treated with chelex 100 resin (Bio-Rad Laboratories) before use to remove metals.

For determination of hydrogen peroxide levels, colons were dissected, cut into small pieces, suspended in phosphate-buffered saline, and incubated for 30 min at room temperature with rotation. After centrifugation, the supernatants were applied to the NWLSS NWK-HYP01 assay kit (Northwest Life Science Specialties, LLC, Vancouver, WA).

Determination of the Amount of PC-SOD and TNF-α in Vivo. Determination of the amount of PC-SOD was carried out as described previously (Igarashi et al., 1992). After administration of PC-SOD, the blood was collected, and serum samples were obtained by centrifugation. On the other hand, colons were dissected, cut into small pieces, homogenized, and centrifuged to obtain the supernatants. Samples were analyzed using a human Cu/Zn-SOD enzyme-linked immunosorbent assay (ELISA) kit (Bender MedSystems Inc., Burlingame, CA). We used PC-SOD (or U-SOD) for drawing the standard curve of ELISA and determined the amount of PC-SOD (or U-SOD). The amount of TNF-α in serum was determined similarly by use of its ELISA kit from Pierce Chemical (Rockford, IL).

Preparation of Mouse Peritoneal Macrophages. Mouse peritoneal macrophages were prepared as described previously (Salimuddin et al., 1999). Mice were given 2 ml of 10% enzymatic digest of animal tissue by intraperitoneal injection, and peritoneal cells were harvested 3 days later. The cells were seeded in 60-mm culture dishes at 4×10^6 cells/dish in RPMI 1640 medium supplemented with 10% heat-inactivated fetal bovine serum. After incubation for 4 h, nonadherent cells were removed, and the adherent cells were cultured for use in the experiments. Virtually all of the adherent cells were macrophages, as previously described (Salimuddin et al., 1999).

Statistical Analysis. All values are expressed as the mean ± S.E.M. Two-way analysis of variance followed by the Tukey test or the Student's *t* test for unpaired results were used to evaluate differences between more than three groups or between two groups, respectively. Differences were considered to be significant for values of $P < 0.05$.

Results

A Comparison of the Effect of PC-SOD and U-SOD on DSS-Induced Colitis. The severity of DSS-induced colitis can be monitored by various indices, such as DAI, length of colon, MPO activity, and histological analysis. We compared PC-SOD and U-SOD for their effect on the development of colitis induced by 4% DSS administration. The clinical study was performed with 40 and 80 mg PC-SOD (Suzuki et al., 2008b), which corresponds to 2 and 4 kU/kg; therefore, we chose the dose of 3 kU/kg for the following experiments. PC-SOD and U-SOD were intravenously administered once daily. There was no significant difference in the volume of water consumed by each group of mice (data not shown). Administration of 4% DSS increased the DAI, and this increase was significantly suppressed by the administration of PC-SOD (3 kU/kg) but not U-SOD (3 kU/kg) (Fig. 1A). DSS-induced colon shortening, used as a morphometric measure for the degree of inflammation, was significantly ameliorated

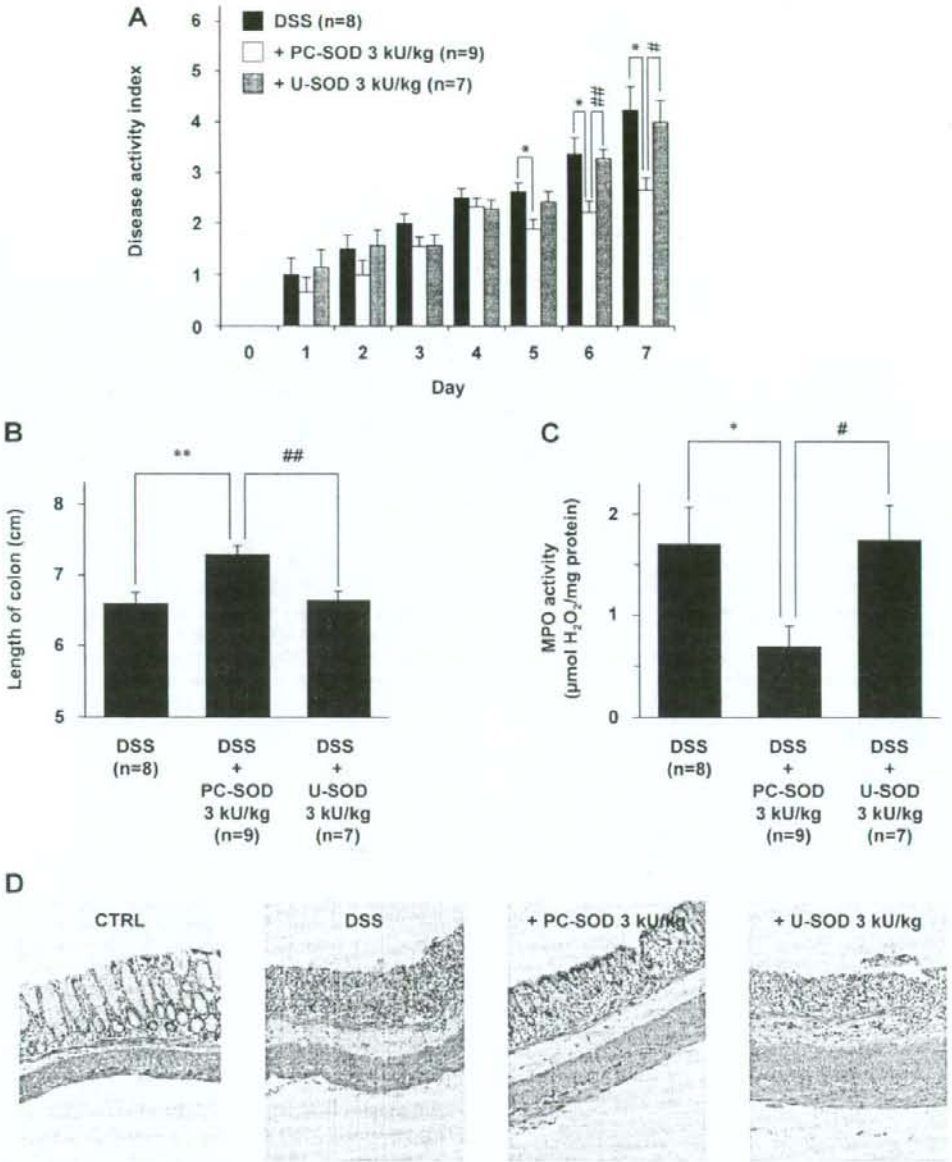

Fig. 1. Effect of PC-SOD and U-SOD on development of DSS-induced colitis. Mice treated with 4% DSS for 7 days, as described under *Materials and Methods*, were intravenously administered PC-SOD or U-SOD once daily. DAI was measured daily (A). The length of the colon (B) and colonic MPO activity (C) were determined at the end of the experimental period. Sections of colonic tissue were also prepared and subjected to histological examination by hematoxylin and eosin staining (D). CTRL, control without DSS treatment. Values are mean ± S.E.M. * or #, $P < 0.05$; ** or ##, $P < 0.01$.

in the PC-SOD-treated animals (Fig. 1B), as was colonic MPO activity, an indicator of leukocyte infiltration (Fig. 1C). Figure 1D shows the results of histological analyses of colonic tissues. Crypt loss and infiltration of leukocytes were observed in DSS-treated mice, and these phenotypes were improved by administration of PC-SOD and, to a lesser extent, U-SOD (Fig. 1D). Taken together, these findings demonstrate that PC-SOD is more effective than U-SOD for the amelioration of DSS-induced colitis.

To compare the specific activity of PC-SOD and U-SOD, we determined their dose-response profiles. As shown in Fig. 2A, PC-SOD produced the maximum beneficial effect at 1.5 to 3 kU/kg, whereas higher doses (6–12 kU/kg) had no significant effect on DAI. A similar bell-shaped profile has also been reported in a rat model of DSS-induced colitis (Hori et al., 1997). In the case of colon shortening and colonic MPO activation, the maximal effect was again observed in response to 1.5 to 3 kU/kg PC-SOD (Fig. 2, B and C). In contrast, U-SOD at the much higher concentration of 48 kU/kg only ameliorated DSS-induced colitis to a similar extent to that obtained